

Volume Osmotic Flows of Non-Homogeneous Electrolyte Solutions through Horizontally Mounted Membrane

A. ŚLĘZAK^{1,4}, J. JASIK-ŚLĘZAK¹, J. WĄSIK², A. SIEROŃ³ AND W. PILIS⁴

1 Department of Economical Analysis and Logistic, Technical University of Częstochowa, Armii Krajowej 19B, PL-42200 Częstochowa, Poland

2 Institute of Physics, Pedagogical University, Częstochowa, Poland

3 Chair and Clinic of Internal Disease and Physical Medicine, Silesian Medical University, Batorego 15, PL-41902 Bytom, Poland

4 Department of Physiology, Academy of Physical Education, Mikołowska 72a, PL-40065 Katowice, Poland

Abstract. Results of an experimental study of volume osmotic flows in a single-membrane osmotic-diffusive cell, which contains a horizontal, microporous, symmetrical polymer membrane separating water and binary or ternary electrolyte solutions are presented. In the experimental set-up, water was placed on one side of the membrane. The opposite side of the membrane was exposed to binary or ternary solutions. As binary solutions, aqueous potassium chloride or ammonia solutions were used, whereas potassium chloride in $0.25 \text{ mol}\cdot\text{l}^{-1}$ aqueous ammonia solution or ammonia in $0.1 \text{ mol}\cdot\text{l}^{-1}$ aqueous potassium chloride solution were used as ternary solutions. Two (A and B) configurations of a single-membrane osmotic-diffusive cell in a gravitational field were studied. In configuration A, water was placed in a compartment above the membrane and the solution below the membrane. In configuration B the position of water and solution was reversed. Furthermore, the effect of amplification of volume osmotic flows of electrolyte solutions in the single-membrane osmotic-diffusive electrochemical cell was demonstrated. The thermodynamic models of the flux graviosmotic and amplification effects were developed, and the volume flux graviosmotic effect for configurations A and B of a single-membrane osmotic-diffusive cell was calculated. The results were interpreted within the conventional instability category, increasing the diffusion permeability coefficient value for the system: concentration boundary layer/membrane/concentration boundary layer.

Key words: Membrane transport — Concentration boundary layers — Amplification — Gravity effects

Correspondence to: Dr. Jacek Wąsik, Institute of Physics, Pedagogical University, Armii Krajowej 13/15, PL-42200 Częstochowa, Poland. E-mail: j.wasik@wsp.czyst.pl

Introduction

The transport of soluble substances and water in membrane systems is attracting great interest in many fields of technology (Rautenbach and Albert 1989) where membranes are used as filters, and also in biophysics (Thornley 1976), where transmembrane transport plays a crucial role in cell physiology. Membrane transport across biological (Dainty 1963; Dainty and Hause 1966; Thomson and Dietchy 1977; Barry and Diamond 1984; Cotton and Reuss 1989) as well as across polymer membranes (Ginzburg and Katchalsky 1963; Hwang and Kammermeyer 1981; Havstein 1987; Bhattacharya and Hwang 1997) separating solutions of different compositions leads to the formation of concentration boundary layers (CBLs). These layers are regions in the external solutions, adjacent to the membrane interfaces, where concentration gradients are maintained under steady-state conditions. CBLs act as pseudo-membranes in series with the physical membrane. Consequently, they can cause substantial reductions in the osmotic and diffusion transmembrane fluxes (Ślęzak and Dworecki 1984). Gravitational force exerts a relatively strong influence on thermodynamic systems and is one of the factors modifying transmembrane transport. Of special interest is the formation of CBL on both sides of horizontally mounted polymer membranes. Under terrestrial conditions, gravitational force has an ambiguous influence on the thickness of these layers; it also decreases the value and changes distributions of solution concentrations occurring (Ślęzak et al. 1985; Ślęzak 1989; Dworecki 1995). The osmotic and diffusion fluxes were significantly higher when the denser liquid was below the membrane in a horizontally mounted osmotic-diffusion cell (Ślęzak et al. 1985; Ślęzak 1989). They explained this observation in terms of natural convection instability that reduced CBL thickness. These CBLs are thick and thus solution concentration decreases markedly in them. It is a different case altogether in layers on which the force of gravity (FG) has a destructive influence, e.g. when the denser liquid is above membrane. These layers are thinner, and the reductions in solution concentration are relatively small (Dworecki 1995; Dworecki and Wąsik 1997). Vigorous mechanical stirring of the external solutions minimises the CBL thickness and transmembrane flux reduction (Inenaga and Yoshida 1980; Ślęzak and Dworecki 1984).

FG influences the kinetics of movement of both ions and non-dissociated molecules through the cellular membrane. This influence is dependent on the dimension of molecules or ions, the charge of ion and density gradient of solution near the membrane. In case of relatively large molecules or ions this influence manifests in the form of sedimentation. One of the models that explain the influence of FG on the cell, is the Schatz's model (Schatz and Linke-Hommes 1989; Schatz et al. 1992). This model is based on the assumption that FG could act on a biological cell by inducing an adaptation provoked through physico-chemical changes in the cellular environment. These changes are caused by lack of sedimentation and natural convection in the cell under microgravity conditions. The lack of these phenomena has produced an influence on nutrition, oxygen and by-product gradients, because in states of microgravity these elements are only produced by diffusion. In this con-

nection Schatz and co-workers (Schatz and Linke-Hommes 1989; Schatz et al. 1992) infer that in conditions of microgravity in the cell-solution border the membrane potential changes could occur causing alterations of solution concentration hence leading to the formation of stationary boundary layers around the cell. This means that in the cells, in which the rate of both oxygen and nourishment consumption exceeds diffusion rate, cell metabolism could be distinctly disturbed (Cogoli and Gründer 1991).

The study of the CBLs formation may be realised in artificial systems under terrestrial conditions by using the single- or double-membrane osmotic-diffusive electrochemical cell. In the single-membrane osmotic-diffusive cell, the influence of FG on ion transport and its distribution on both sides of the membrane is manifested by means of membrane potential, ionic current as well as osmosis and diffusion (Ślęzak 1989, 1990, 1997; Pohl et al. 1997; Ślęzak et al. 2000a). The influence of the gravitational force on the passage of uncharged particles through membranes is demonstrated is only by osmosis and diffusion (Ślęzak 1989). In the double-membrane osmotic-diffusive cell the main phenomenon is graviosmosis (Przestalski and Kargol 1987; Kargol 1994). Graviosmosis consists of generating proper volume flows in an osmotically symmetric double-membrane cell. It is caused by reorientation of such a cell with respect to direction of FG. This phenomenon is the foundation of the so-called graviosmotic hypothesis of xylem water-uptake in plants (Kargol 1992).

As a result of diffusion and osmosis on both sides of a membrane, separating two mechanically unstirred solutions, different CBLs are created. The CBLs are the areas immediately adjacent to the membrane surface area and can be treated as a pseudomembrane (Pedley and Fischbarg 1978, 1980; Pedley 1983; Barry and Diamond 1984). The solution in boundary layer areas does not change its location and is adjacent to the laminar movement area, in which the natural convection does not cause substantial mixing of the solution. The thickness of this layer depends on the type of solutions used, their composition, concentrations and densities, and on the orientation of the membrane and the measurement chamber containing solution relative to the gravitational vector (Barry and Diamond 1984; Ślęzak et al. 1985; Ślęzak 1989; Dworecki 1995). Stirring of the solution causes a decrease in the concentration boundary layer thickness. However, even vigorous stirring does not cause entire decay of the boundary layer (Inenaga and Yoshida 1980). The directly observed CBLs creation in different configurations of a single-membrane system manifested by: 1. bending of interference stripes in the area near the membrane received on interferograms by means of the Mach-Zehnder interferometer (Lerche and Wolf 1971; Lerche 1976; Ślęzak et al. 1985; Dworecki 1995; Dworecki and Wąsik 1997), 2. decrease in the volume and solute fluxes (Ślęzak 1989; Ślęzak et al. 2000b) and 3. decrease in the diffusive membrane potential (Ślęzak 1990). The influence of the gravitational field on the transmembrane flow can be demonstrated by measurements in a steady state of thermodynamic fluxes or forces when the solutions are well stirred and when the solutions are unstirred (Ślęzak et al. 2000a). The influence of FG on the passive transmembrane transport lead to the graviosmotic

(flux and force), gravidiffusive (flux and force) and gravelectric (flux and force) (Ślęzak et al. 2000a) effects.

The present paper presents experimental results of an osmotic volume flux study in two different configurations (A and B) of a single-membrane osmotic-diffusive electrochemical cell containing a horizontally mounted membrane under conditions of mechanical stirring and without mechanical stirring of binary or ternary electrolyte solutions. A flat polymer membrane and aqueous solutions of potassium chloride and/or ammonia were used. On this basis volume flux graviosmotic effects were calculated. Using an irreversible thermodynamic method, model equations of the volume flux graviosmotic effect for a single-membrane osmotic-diffusive cell were developed. In order to test this model, both experimental and calculation results for volume osmotic flux in a single-membrane osmotic-diffusive cell containing binary and ternary electrolyte solutions are presented. The effect of amplification of the osmotic volume flows of electrolyte solutions in a single-membrane osmotic-diffusive cell is described.

Membrane system

Let us consider configurations A_r and B_r ($r = 1, 2$) of a single-membrane system represented in Fig. 1. In this system the compartments (l) and (h) contain dilute and non-homogeneous (mechanically unstirred) multicomponent solutions of the same electrolyte with concentrations equal to C_s^l and C_s^h . They are separated by isotropic, symmetrical, selective and electroneutral membrane (M). These concentrations satisfy the condition that $C_s^l < C_s^h$. The solution contains s ($s = 1, 2$) uninteracting substances dissolved in solvent w . The initial concentrations (at time $t = 0$) of these solutions are denoted by C_1^l , C_1^h , C_2^l and C_2^h . In both configurations, the membrane M is oriented in a horizontal plane with the corresponding concentration gradients being antiparallel and parallel to the gravitational vector. The transport process is isothermal and stationary, and no chemical reactions are occurring in the solutions. The membrane is characterised by hydraulic permeability (L_p), reflection (σ_s) and diffusion permeability (ω_{ks}) coefficients.

At $t > 0$, in this system, water and the dissolved substances diffusing across the membrane lead to the formation of CBLs. These layers can be treated as pseudo-membranes. The reflection and diffusive permeability coefficients of the complexes: concentration boundary layer/membrane/concentration boundary layer (CBL/M/CBL) are denoted by σ_s^i and Ω_{ks}^i , respectively. Within the CBLs, the concentration of a solute is a function of the distance from the membrane, and it is not equal to that in the bulk solution. The effect of the CBL is assessed based on the assumption that the only motion in the CBL is the osmotic flux itself, and C depends only on the distance x from the membrane (Dainty 1963).

The thicknesses of the layers δ_1^i and δ_h^i are defined in terms of the concentration gradient at the membrane-water and membrane-solutions interfaces, respectively (Dainty and House 1966)

$$\frac{|(C_s^1)^i - C_s^1|}{\delta_1^i} = \left. \frac{\partial C_s^1}{\partial x} \right|_{x \neq 0} \quad (1)$$

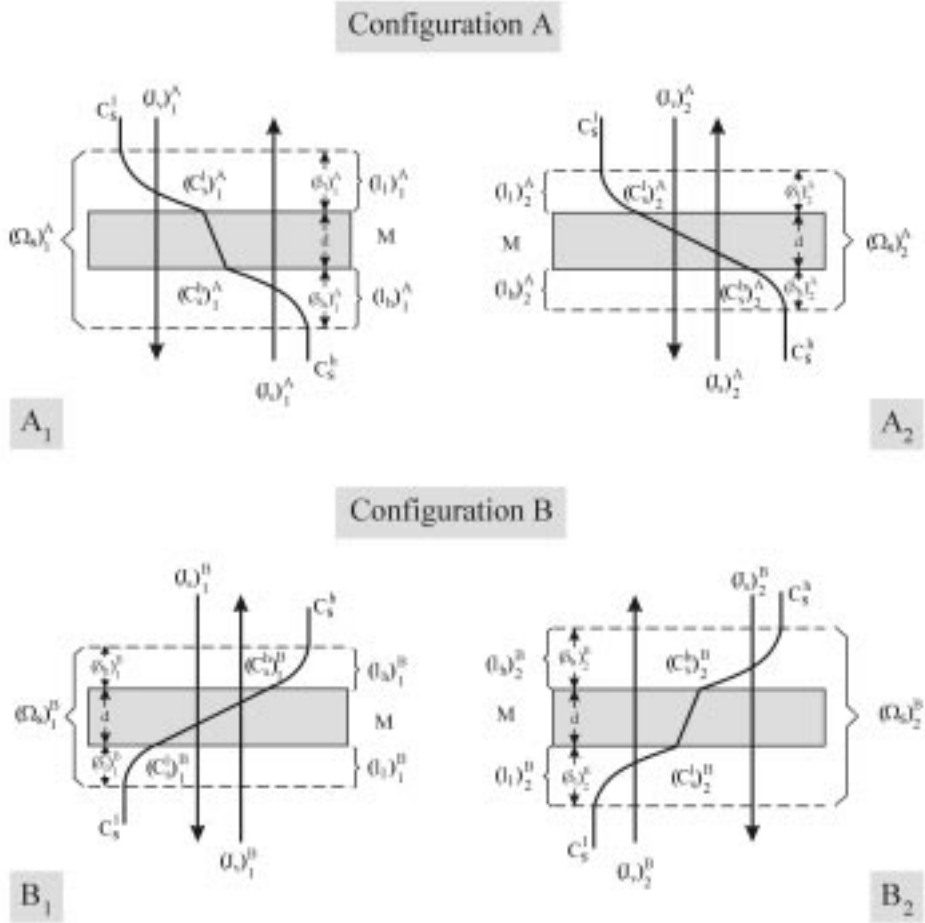


Figure 1. Graphic illustration of configurations A and B of the single-membrane osmotic-diffusive cell and concentration profiles A₁, A₂, B₁ and B₂ (stable A₁ and B₂ and unstable A₂ and B₁). (M, membrane; d, thicknesses of the membrane; $l_1^{A_1}, l_h^{A_1}, l_1^{A_2}, l_h^{A_2}, l_1^{B_1}, l_h^{B_1}, l_1^{B_2}, l_h^{B_2}$ – concentration boundary layers; $\delta_1^{A_1}, \delta_h^{A_1}, \delta_1^{A_2}, \delta_h^{A_2}, \delta_1^{B_1}, \delta_h^{B_1}, \delta_1^{B_2}, \delta_h^{B_2}$ – thickness of the boundary layers; C_s^l, C_s^h – global solution concentrations; $(C_s^l)^{A_1}, (C_s^h)^{A_1}, (C_s^l)^{A_2}, (C_s^h)^{A_2}, (C_s^l)^{B_1}, (C_s^h)^{B_1}, (C_s^l)^{B_2}, (C_s^h)^{B_2}$ – local solution concentrations on boundaries membrane-boundary layers; $J_{vs}^{A_1}, J_{vs}^{A_2}, J_{vs}^{B_1}, J_{vs}^{B_2}$ – volume fluxes; $J_s^{A_1}, J_s^{A_2}, J_s^{B_1}, J_s^{B_2}$ – dissolved substance fluxes; $\Omega_{ks}^{A_1}, \Omega_{ks}^{A_2}, \Omega_{ks}^{B_1}, \Omega_{ks}^{B_2}$ – diffusive permeability coefficients of the complex: boundary layer/membrane/boundary layer).

$$\frac{|C_s^h - (C_s^h)^i|}{\delta_h^i} = \left. \frac{\partial C_s^h}{\partial x} \right|_{x=0} \quad (2)$$

where: x is the distance from the membrane, C_s^h and C_s^l represent the solute con-

centrations in the compartment h and l respectively, $(C_s^h)^i$ and $(C_s^l)^i$ denote the solute concentrations at the interfaces, index $i = A_r, B_r$; $s = 1, 2$; $r = 1, 2$.

Let us consider the configurations A_1 and B_2 schematically represented in the Fig. 1. These configurations illustrate the situation in which the solution with higher density is above the membrane, and the one with lower density – below the membrane. The configurations A_2 and B_1 illustrate the situation in which the solution with lower density is above the membrane and the solution with higher density below the membrane. Assuming that concentrations C_s^h and C_s^l are stationary, should the solution density be directly proportional to the concentration, configurations A_1 and B_1 are possible. This situation is typical for aqueous solutions of glucose, saccharose, KCl or NaCl. However, should the solution density be inversely proportional to the concentration, configurations A_2 and B_2 are possible. This situation can occur in aqueous solutions of first-row alcohols (ethanol, methanol) and ammonia. In ternary solutions, if the concentration of component decreasing density of solution is constant, then increase in concentration of component increasing density causes that density of the solution in the chamber below the membrane in configuration A can be lower, equal or higher than the density of water. If the density of solution in the chamber above the membrane is lower than the density of solution in the chamber below the membrane, then the concentration profile is similar to that in configurations A_1 or B_2 . If the density of solution in the chamber above the membrane is higher than the density of solution in the chamber below the membrane, the concentration profile is likewise to that in configurations A_2 or B_1 .

In A_2 and B_1 configuration the process of layers $l_1^{A_2}, l_h^{A_2}, l_1^{B_1}, l_h^{B_1}$ formation is finished at the moment of appearance of natural convection and attains the stationary state by osmotic-diffusion cell. Then the thicknesses of layers: $\delta_1^{A_2}, \delta_h^{A_2}, \delta_1^{B_1}, \delta_h^{B_1}$ are constant, because possible increase in thickness is limited by natural convection. In this connection, the concentration of solution at boundaries of membrane-solution increases from C_s^l to $(C_s^l)^{A_2}$ (in A_2 configuration) or to $(C_s^l)^{B_1}$ (in B_1 configuration) whereas the concentration C_s^h decreases to $(C_s^h)^{A_2}$ (in A_2 configuration) or to $(C_s^h)^{B_1}$. Besides, $(C_s^l)^{A_1} > (C_s^l)^{B_1}$, $(C_s^h)^{A_1} < (C_s^h)^{B_2}$, $(C_s^l)^{A_2} < (C_s^l)^{B_1}$ and $(C_s^h)^{A_2} > (C_s^h)^{B_2}$. The volume and solute fluxes in configuration A_2 are represented by $J_{v_s}^{A_2}$ and $J_s^{A_2}$. In configuration B_1 , the volume and solute fluxes are represented by $J_{v_s}^{B_1}$ and $J_s^{B_1}$.

In A_1 and B_2 configurations there is no natural convection near the membrane. Therefore, the process of layers $l_1^{A_1}, l_h^{A_1}, l_1^{B_2}, l_h^{B_2}$ formation is finished in a state of thermodynamic equilibrium, because the thickness of these layers constantly increases. This is well-founded by inverted gradient of solution density. However, we can assume that in a state when $J_{v_s}^i = \text{const.}$ and $J_s^i = \text{const.}$, the thicknesses of these layers are $\delta_1^{A_1}, \delta_h^{A_1}, \delta_1^{B_2}$ and $\delta_h^{B_2}$. The value of thickness of CBL formed on both sides of a horizontally mounted membrane can be determined using the Nernst criterion (Nernst 1904) based on distribution curves of concentrations. In this connection in the stationary state of membrane transport, solution concentration at boundaries between membrane and solution reaches values $(C_s^l)^{A_1}$ and

$(C_s^h)^{A_1}$ (in configuration A_1) and $(C_s^l)^{B_2}$ and $(C_s^h)^{B_2}$ (in configuration B_2). Besides, $(C_s^l)^{A_1} > C_s^l$, $(C_s^h)^{A_1} < C_s^h$, $(C_s^l)^{B_2} > C_s^l$ and $(C_s^h)^{B_2} < C_s^h$.

The diffusion permeability coefficients of the complex CBL/M/CBL are denoted suitably by $\Omega_{ks}^{A_1}$, (in configuration A_1), $\Omega_{ks}^{A_2}$ (in configuration A_2), $\Omega_{ks}^{B_1}$ (in configuration B_1) and $\Omega_{ks}^{B_2}$ (in configuration B_2). For binary solutions the values of these coefficients depend only on the configuration of one membrane system; in the stable configuration (A_1, B_2) it is lower than in unstable configuration (A_2, B_1). If the solutions are well stirred then $(C_s^l)^i = C_s^l$, $(C_s^h)^i = C_s^h$, $J_{vs}^i = J_{vs}$, $J_s^i = J_s$, $\delta_1^i = \delta_h^i \cong 0$ and $\Omega_{ks}^i = \omega_{ks}$ ($i = A, B$). In the stationary state, these conditions are satisfied: $J_{vs}^0 = \text{const.}$, $J_{vs}^i = \text{const.}$, $J_s^0 = \text{const.}$, and $J_s^i = \text{const.}$

For the case presented in Figure 1, Van't Hoff's law can be expressed as follows:

$$\Delta\Pi_s = RT(C_s^h - C_s^l) \quad (3)$$

$$\Delta\Pi_s^i = RT[(C_s^h)^i - (C_s^l)^i] \quad (4)$$

where: RT is the product of the gas constant and absolute temperature, C_s^h and C_s^l the global (in the bulk) solutions concentration, $(C_s^h)^i$ and $(C_s^l)^i$ the local (at the interfaces) solutions concentration, index $i = A_r, B_r$ ($r = 1, 2$) pertain to configurations A and B respectively.

Model equations of the volume osmotic flux

The basic manner of describing of membrane transport processes of homogeneous electrolyte solutions, originated from nonequilibrium thermodynamics of irreversible processes, is the Kedem-Katchalsky model equations. In the case of osmotic membrane transport of ternary electrolyte solutions this model is represented by the equation (Katchalsky and Curran 1965)

$$J_{vs}^0 = L_p \left(\sum_{s=1}^2 \sigma_s \zeta_s \Delta\Pi_s \pm \Delta P \right) \quad (5)$$

where: σ_s^s is the volume osmotic flux, L_p is the hydraulic permeability coefficient of the membrane, ζ_s is the Van't Hoff coefficient ($1 \leq \zeta_s \leq 2$, for non-electrolyte solutions $\zeta_s = 1$), ΔP is the hydrostatic pressure difference, $\Delta\Pi_s = RT(C_s^h - C_s^l)$, $C_s^h > C_s^l$ is the osmotic pressure difference, RT is the product of gas constant and thermodynamic temperature, $\bar{C}_s = (C_s^h - C_s^l)[\ln(C_s^h/C_s^l)]^{-1} \approx 0.5(C_s^h + C_s^l)$ is the mean solution concentration, σ_s is the reflection coefficient of the membrane, ω_{ks} is the diffusion permeability coefficient of the membrane for s -th substance, permeating through the membrane thanks to the osmotic pressure difference connected with gradient of k -th substance ($\omega_{ks} = \omega_{sk} \bar{C}_s \cdot \bar{C}_k^{-1}$; $s = 1, 2$).

This model is valid in cases, where: 1. the membrane divides two ternary solutions consisting of two mutually independent substances dissolved in solvent w; 2. the membrane is selective, homogeneous and electrically indifferent and has a finite thickness; 3. the solutions are diluted and homogeneous, that is to say that the gradient of chemical potential occurs only at the membrane. In the solutions,

chemical reactions do not occur and processes of membrane transport are isothermal.

In order to assure solution homogeneity, mechanical stirring of solutions should be used, propelled by an external force with a suitably fitted shear rate. This procedure is possible only in artificial systems. In the biological systems, however, the condition of homogeneity is not satisfied, similar to the artificial systems without the mechanical stirring of solutions. If the solutions are not mechanically stirred, then concentration boundary layers are formed on both sides of the membrane. The boundary layers are the fluid areas adjoined to the membrane surface and possess a pseudo-membrane property, connected with the membrane in series (Barry and Diamond 1984).

The modified Kedem-Katchalsky model equation (Ślęzak et al. 1989) is the basic manner of describing membrane transport processes of non-homogeneous electrolyte solutions, originated from non-equilibrium thermodynamics of irreversible processes. In the case of osmotic membrane transport of ternary electrolyte solutions this model is expressed by the equation:

$$J_{vs}^i = \xi_v^i \left((\det K)^{-1} \sum_{s=1}^2 \zeta_s \gamma_s^i \Delta \Pi_s \pm \Delta P \right) \quad (6)$$

where:

$$\xi_{vs}^i = L_p \left[1 + (\det K)^{-1} L_p \left(\sum_{s=1}^2 \sigma_s \det M_s^i \right) \right]^{-1},$$

$$\det K = \omega_{11}\omega_{22} - \omega_{21}\omega_{12},$$

$$\det M_1^i = \omega_{22}[\bar{C}_1^i(1 - \sigma_1^i) - (1 - \sigma_1)\bar{C}_1] - \omega_{21}[\bar{C}_2^i(1 - \sigma_2^i) - (1 - \sigma_2)\bar{C}_2],$$

$$\det M_2^i = \omega_{11}[\bar{C}_2^i(1 - \sigma_2^i) - (1 - \sigma_2)\bar{C}_2] - \omega_{12}[\bar{C}_1^i(1 - \sigma_1^i) - (1 - \sigma_1)\bar{C}_1],$$

$$\gamma_1^i = \sigma_1 \det K_{11}^i + \sigma_2 \det K_{21}^i,$$

$$\gamma_2^i = \sigma_1 \det K_{21}^i + \sigma_2 \det K_{22}^i,$$

$$\det K_{12}^i = \omega_{22}\Omega_{21}^i - \omega_{21}\Omega_{22}^i,$$

$$\det K_{21}^i = \omega_{11}\Omega_{12}^i - \Omega_{11}^i\omega_{12},$$

$$\det K_{11}^i = \Omega_{11}^i\omega_{22} - \omega_{21}\Omega_{12}^i,$$

$$\det K_{22}^i = \omega_{11}\Omega_{22}^i - \Omega_{21}^i\omega_{12},$$

$\bar{C}_s^i = [(C_s^h)_k^i - (C_s^l)_k^i] \{ \ln [(C_s^h)_k^i / (C_s^l)_k^i] \}^{-1} \approx 0.5 [(C_s^h)_k^i + (C_s^l)_k^i]$ is the mean concentration of solution, ζ_s is the Van't Hoff coefficient, σ_s^i is the reflection coefficient of the complex CBL/M/CBL, Ω_{ks}^i is the diffusion permeability coefficient of the complex CBL/M/CBL for s -th substance, permeating through the membrane thanks to osmotic pressure difference connected with gradient of k -th substance ($\Omega_{ks}^i = \Omega_{sk}^i \cdot \bar{C}_s \cdot \bar{C}_k^{-1}$; $s = 1, 2$; $s \neq k$).

The definitions and interpretation of the phenomenological coefficients of the membrane transport for ternary solutions (L_p , σ_s , σ_s^i , ω_{ks} , Ω_{ks}^i) were presented in previous papers (Ślęzak 1989; Ślęzak et al. 1989). In these papers it was shown that the values of coefficients σ_s^i and Ω_{ks}^i for binary and ternary solutions may be a function of the configuration of the single-membrane system and the values of σ_s^i and Ω_{ks}^i for ternary solutions are a function of the concentration of the solutions.

For coefficients Ω_{ks}^i , ω_{ks} the next relation applies (Ginzburg and Katchalsky 1963)

$$\frac{1}{\Omega_{ks}^i} = \frac{1}{\omega_{ks}} + \frac{RT}{D_{ks}^i}(\delta_1^i + \delta_h^i) \quad (7)$$

where: D_{ks}^i is the coefficient of solute diffusion in solution, δ_1^i and δ_h^i are the thicknesses of concentration boundary layers suitably in compartments l and h in i -th configurations ($i = A, B$).

Model equation of the volume flux graviosmotic effect

The volume flux graviosmotic effect ($jGOE$) $_s^i$ was determined on the basis of the measured values of J_{vs}^0 and J_{vs}^i ($i = A, B$) using the following equation (Ślęzak et al. 2000a)

$$(jGOE)_s^i = J_{vs}^0 - J_{vs}^i \quad (8)$$

Taking into consideration equations (5) and (6) in equation (8) we hence derive

$$(jGOE)_s^i = \sum_{s=1}^2 [L_p \sigma_s - (\det K)^{-1} \zeta_s \xi_{vs}^i \gamma_s^i] \zeta_s \Delta \Pi_s + (\xi_{vs}^i - L_p) \Delta P \quad (9)$$

Materials and Methods

Studies of osmotic volume flows were carried out by means of the measuring apparatus whose detailed description was given in a previous paper (Ślęzak and Dworecki 1984). The apparatus consisted of two Plexiglas vessels (l, h) separated by membrane (M) with equal active surface area of $3.36 \pm 0.2 \text{ cm}^2$ and a thickness of $200 \pm 10 \text{ }\mu\text{m}$ in the hydrated state. The membrane was mounted in a horizontal plane. The experiments were performed with a flat sheet *Nephrophane* (cellulose acetate) hemodialyzer membrane. Parameters of the membrane, i.e. hydraulic permeability (L_p), reflection (σ_s) and diffusive permeability (ω_{ks}) coefficients of the membrane, and the reflection (σ_s^i) and diffusive permeability (Ω_{ks}^i) coefficients of the complex (CDL/M/CDL) have been determined for configurations A $_r$ and B $_r$ in accordance with methods described in previous papers (Katchalsky and Curran 1965; Ślęzak 1989). Their values for the *Nephrophane* membrane and for binary aqueous potassium chloride and ammonia solutions are listed in Table 1. The values of densities of aqueous solutions of potassium chloride and/or ammonia (ρ_1 , ρ_2) are listed in Table 2. The values of all these coefficients do not depend on the solution concentration for dilute binary solutions, whereas values of the coefficients Ω_{ks}^i for ternary

Table 1. Values of the *Nephrophane* flat dialysis membrane transport parameters for potassium chloride (subscript 1) and ammonia (subscript 2)

Coefficient	Value of parameter	
	Configuration A	Configuration B
$L_p \cdot 10^{12} [\text{m}^3 \cdot \text{N}^{-1} \cdot \text{s}^{-1}]$	5.0 ± 0.2	5.0 ± 0.2
$\sigma_1 \cdot 10^2$	4.0 ± 0.1	4.0 ± 0.2
$\sigma_2 \cdot 10^2$	1.00 ± 0.02	1.00 ± 0.02
$\sigma_1^i \cdot 10^3$	0.50 ± 0.01	9.6 ± 0.1
$\sigma_2^i \cdot 10^4$	2.90 ± 0.02	0.40 ± 0.01
$\omega_{11} \cdot 10^{10} [\text{mol} \cdot \text{N}^{-1} \cdot \text{s}^{-1}]$	2.5 ± 0.1	2.5 ± 0.1
$\omega_{22} \cdot 10^9 [\text{mol} \cdot \text{N}^{-1} \cdot \text{s}^{-1}]$	2.68 ± 0.02	2.68 ± 0.02
$\omega_{12} \cdot 10^{13} [\text{mol} \cdot \text{N}^{-1} \cdot \text{s}^{-1}]$	6.1 ± 3.5	6.1 ± 3.5
$\omega_{21} \cdot 10^{12} [\text{mol} \cdot \text{N}^{-1} \cdot \text{s}^{-1}]$	1.6 ± 0.6	1.6 ± 0.6
$\Omega_{11}^i \cdot 10^{10} [\text{mol} \cdot \text{N}^{-1} \cdot \text{s}^{-1}]$	0.03 ± 0.01	0.6 ± 0.2
$\Omega_{22}^i \cdot 10^9 [\text{mol} \cdot \text{N}^{-1} \cdot \text{s}^{-1}]$	0.78 ± 0.06	0.01 ± 0.02
$\Omega_{12}^i \cdot 10^{13} [\text{mol} \cdot \text{N}^{-1} \cdot \text{s}^{-1}]$	2.5 ± 0.3	0.20 ± 0.05
$\Omega_{21}^i \cdot 10^{12} [\text{mol} \cdot \text{N}^{-1} \cdot \text{s}^{-1}]$	0.3 ± 0.1	2.0 ± 0.6

Table 2. The values of densities (ρ_1, ρ_2) of aqueous solutions of potassium chloride and/or ammonia

C_1 [mol·l ⁻¹]	$\rho_1 [10^{-3} \cdot \text{kg} \cdot \text{m}^{-3}]$		C_2 [mol·l ⁻¹]	$\rho_2 [10^{-3} \cdot \text{kg} \cdot \text{m}^{-3}]$	
	$C_2 = 0$ [mol·l ⁻¹]	$C_2 = 0.25$ [mol·l ⁻¹]		$C_1 = 0$ [mol·l ⁻¹]	$C_1 = 0.1$ [mol·l ⁻¹]
0.00	0.9980	0.9950	0.0	0.9980	1.0028
0.05	1.0004	0.9974	0.2	0.9954	1.0002
0.10	1.0028	0.9998	0.4	0.9928	0.9976
0.15	1.0052	1.0022	0.6	0.9902	0.9950
0.20	1.0076	1.0046	0.8	0.9876	0.9924
0.25	1.0100	1.0070	1.0	0.9850	0.9898
0.30	1.0124	1.0094	1.2	0.9824	0.9872

Index 1, potassium chloride; index 2, ammonia; C_1 , concentration of potassium chloride; C_2 , concentration of ammonia.

solutions do, as is shown in Figs. 7 and 8. Volumes of the vessels (l, h) were the same and equal to 200 cm³. The vessel (h) contained aqueous potassium and/or ammonia solution at varied concentrations, whereas the vessel (l) was filled with pure water in all the experiments. The vessel (h) was coupled with a calibrated pipette, which allowed measurements of the volume with accuracy $\pm 0.5 \text{ mm}^3$, while the vessel (l) was connected to an external reservoir of pure water at the same height as the

pipette. The stirring speed in each chamber was maintained at approximately 500 rpm using independently controlled stirrer motors. All experiments were performed at a temperature $T = (295 \pm 0.1)$ K.

The volume flux was measured for gravitational configurations (A_r and B_r) of the membrane system. In configuration A_r , the vessel (1) (containing pure water) was the upper compartment of the single-membrane system, whereas the vessel containing the solution under investigation served as the lower compartment. In configuration B_r , the upper compartment contained the solution, whereas the lower compartment was filled with pure water. The volume flux, J_{vs}^i , was determined from

$$J_{vs}^i = \frac{1}{S} \left(\frac{dV}{dt} \right)^i_{\Delta C_s^i = \text{const}, \Delta P = 0} \quad (10)$$

where: S is the membrane surface area and dV/dt is the volume change (V) occurring in time (t); $i = A_r, B_r$, for A_r and B_r configuration of the system being measured.

Measurements of J_{vs}^0 and J_{vs}^i for both configurations were performed according to the following procedure (Ślęzak 1989). The first step involved the measurement of the volume flux in the single-membrane system by mechanically stirring the solutions at 500 rpm. After achieving the initial steady state during which J_{vs}^0 was constant, stirring was stopped, and subsequently the evolution of volume flux was measured up to the second steady state, while J_{vs}^i remained fixed. The same procedure was followed for each configuration. Each series of measurements was repeated for up to seven times. The concentration dependencies J_{vs}^0 and J_{vs}^i were determined on the basis of time-dependent variability of J_{vs}^0 and J_{vs}^i at a steady state, obtained for different solution concentrations of the same substance and the same configurations of the membrane system. The relative error committed during determination of J_{vs}^i was less than 5%.

The results listed in Table 1 show that *Nephrophan* membrane is selective ($0 < \sigma_s < 1$, $0 < \sigma_s^i < 1$) for both aqueous potassium chloride and ammonia solutions. Moreover, such a membrane undergoes relatively strong concentration polarisation, because of boundary layer creation on both sides of the membrane. Quantitative measure of this effect is the coefficient of concentration polarisation ϑ_{ks}^i specified by the following equation

$$\vartheta_{ks}^i = \frac{\Omega_{ks}^i}{\omega_{ks}} \quad (11)$$

where: $0 \leq \vartheta_{ks}^i \leq 1$, Ω_{ks}^i is the diffusive permeability coefficient of the complex CBL/M/CBL, ω_{ks} is the diffusive permeability coefficient of the membrane. In the case of $\vartheta_{ks}^i = 1$, the membrane does not undergo concentration polarisation. When $\vartheta_{ks}^i = 0$, concentration polarisation of the membrane is maximal. The values of the concentration polarisation coefficients, derived by using formula (11) and Table 1 for binary solutions, amount to: $\vartheta_{11}^A = 0.0125$, $\vartheta_{11}^B = 0.24$, $\vartheta_{22}^A = 0.29$, $\vartheta_{22}^B = 0.004$.

Results

a) Time dependence of volume flux

A typical plot of the time-dependencies of volume osmotic flux (J_{vs}^i) in configurations A_1 and B_1 of the single-membrane system in the case of a $0.1 \text{ mol}\cdot\text{l}^{-1}$ aqueous potassium chloride solution is shown in Fig. 2. The graph 1, common for both configurations, contains the results obtained under conditions of thorough mechanical stirring with 500 rpm, and shows that J_{v1}^0 is independent of the gravitational configuration of the single-membrane system. Graphs 1A and 1B, obtained for configurations A_1 and B_1 respectively, demonstrate that the J_{v1}^i values for both configurations differ. After switching of mechanical stirring of solutions in time $t = 0$, as in configuration A_1 , the flux $J_{v1}^{A_1}$ decreases and after 15 minutes attains a constant value, a little greater than zero. This means that in the stable state of flow, gravitational force almost completely hamper osmotic volume flow. Next in the case of configuration B the flux $J_{v1}^{B_1}$ gains stationary state after 10 minutes and while in the stationary state it is two times lower than flux J_{v1}^0 . The evolution of J_{v1}^0 to $J_{v1}^{A_1}$ or $J_{v1}^{B_1}$ is a reflection of the process of concentration boundary layer

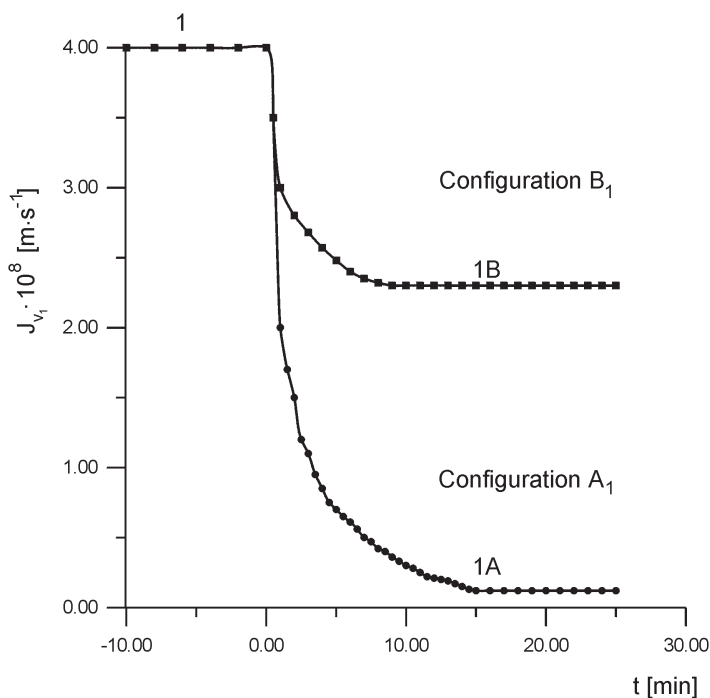


Figure 2. Evolution of the volume flux (J_{vs}^i) from J_{vs}^0 to $J_{vs}^{A_1}$ and $J_{vs}^{B_1}$ in configuration A_1 and B_1 after turning off the mechanical stirrers.

formation on both sides of the membrane. This process stops once the steady state is attained. Thus, we can express that $J_{v1}^0 > J_{v1}^{A_1}$, $J_{v1}^0 > J_{v1}^{B_1}$ and $J_{v1}^{A_1} < J_{v1}^{B_1}$.

b) Concentration dependencies of volume flux

Concentration dependencies of volume flux (J_{vs}^i) for mechanically unstirred binary solutions (aqueous solutions of potassium chloride or ammonia) and ternary solutions (aqueous solutions of potassium chloride and ammonia) for configurations A_1 and B_1 of single-membrane system were illustrated in Figs. 3 and 4. In the Fig. 3, the dependencies of volume flux (J_{v1}^i) on concentration difference of potassium chloride (ΔC_1) with fixed concentration difference of ammonia (ΔC_2), and in the Fig. 4 – on concentration difference of ammonia (ΔC_2) with fixed concentration difference of potassium chloride (ΔC_1) were presented. Index $i = A_1, B_1$ refers to the configurations A_1 and B_1 of the single-membrane system.

The curves 1A and 1B of Fig. 3 were obtained for the situation where $\Delta C_2 = 0$ mol·l⁻¹ (binary solutions), the curves 2A and 2B for $\Delta C_2 = 0.25$ mol·l⁻¹ (ternary solutions). From this figure we deduce that in the binary solution, J_{v1}^i is linearly dependent on ΔC_1 and the values of J_{v1}^i in configuration B_1 are greater than in configuration A_1 . This also means that the values of J_{v1}^i are greater when the solution with a higher density is in the chamber over the membrane, and water is under the membrane.

From the shape of curve 2A we state that flux J_{v1}^i attains a maximum value for: $J_{v1}^{A_1} = 3.8 \times 10^{-8}$ m·s⁻¹ and $\Delta C_1 = 0.05$ mol·l⁻¹. In this case the density of ternary solutions, being in the chamber over the membrane is greater than water density in the chamber under the membrane. For $\Delta C_1 > 0.1$ mol·l⁻¹ the flux $J_{v1}^{A_1}$ is linearly dependent on ΔC_1 , with the same tangent of inclination angle as straight line 1A. In that case the density of ternary solutions in the chamber under the membrane is lower than water density above the membrane. From the course of curve 2B it implies that for $\Delta C_1 < 0.08$ mol·l⁻¹, the value of $J_{v1}^{B_1}$ in a small degree depends on ΔC_1 and ΔC_2 . Therefore the density of ternary solutions in the chamber under the membrane is less than the water density in the chamber above the membrane. For $\Delta C_1 > 0.12$ mol·l⁻¹ the flux $J_{v1}^{B_1}$ is linearly dependent on ΔC_1 with the same tangent of inclination angle as straight line 1B. In this case the density of ternary solutions in the chamber above the membrane is higher than water density in the chamber under the membrane.

In the Fig. 4, the dependencies of volume flux (J_{v2}^i) on the concentration difference of ammonia (ΔC_2) and fixed concentration difference of potassium chloride (ΔC_1) were presented. Index $i = A_2, B_2$ refers to configuration A_2 and B_2 of the single-membrane system. Graphs 1A and 1B were drawn for situation where $\Delta C_1 = 0$ mol·l⁻¹ (binary solutions) and graphs 2A and 2B for $\Delta C_1 = 0.1$ mol·l⁻¹ (ternary solutions). From this figure it results that in the binary solutions J_{v2}^i is linearly dependent on ΔC_2 and in this case the value of J_{v2}^i in configuration A_2 is greater than in B_2 configuration. This also means that the values of J_{v2}^i are greater, when the solution with a higher density is in the chamber above the membrane and water is under the membrane.

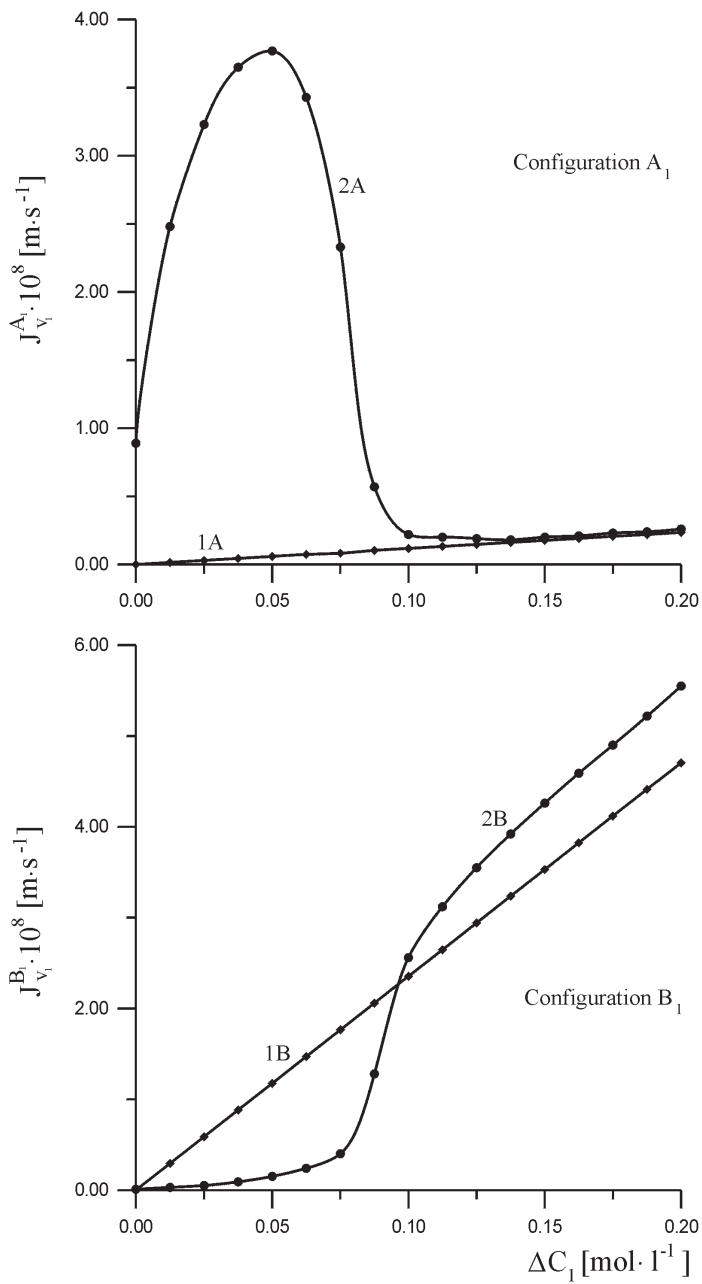


Figure 3. Experimental volume flux (J_{vs}^i) across a single-membrane osmotic-diffusive cell as a function of the potassium chloride concentration difference (ΔC_1) for configuration A₁ (upper) and B₁ (lower) plot: 1(A,B), no ammonia; 2(A,B), $\Delta C_2 = 0.25 \text{ mol}\cdot\text{l}^{-1}$ ammonia. The curves 1(A,B) and 2(A,B) were obtained without any mechanical stirring.

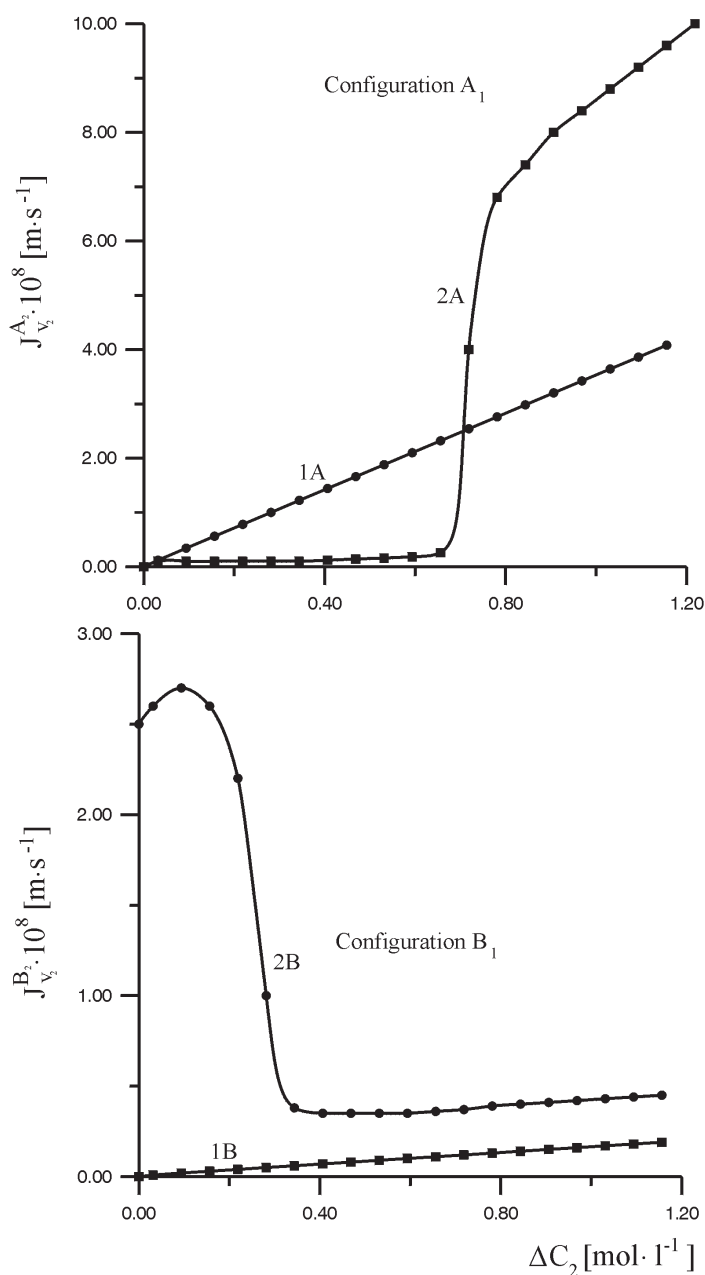


Figure 4. Experimental volume flux (J_{vs}^i) across a cell membrane as a function of the ammonia concentration difference (ΔC_2) for configuration A₂ (upper) and B₂ (lower): curves 1(A,B), no KCl; 2(A,B), $\Delta C_1 = 0.1 \text{ mol}\cdot\text{l}^{-1}$ KCl. All curves in this figure were obtained without any mechanical stirring.

From the slope of curve 2A we notice that when $\Delta C_2 < 0.65 \text{ mol}\cdot\text{l}^{-1}$ the value of J_{v2}^{A2} to a small degree depends on ΔC_2 and ΔC_1 . Therefore this means that the density of ternary solution in the chamber above the membrane is less than the water density in the chamber under the membrane. For $\Delta C_2 > 0.7 \text{ mol}\cdot\text{l}^{-1}$ the flux J_{v2}^{A2} is linearly dependent on ΔC_2 with a tangent of inclination angle two times greater than for line 1A. In this case the density of ternary solution in the chamber above the membrane is greater than water density in the chamber under the membrane. From the slope of curve 2B we conclude that the flux J_{v2}^i reaches its maximum when: $J_{v2}^{B2} = 2.5 \times 10^{-8} \text{ m}\cdot\text{s}^{-1}$ and $\Delta C_2 = 0.1 \text{ mol}\cdot\text{l}^{-1}$. Here the density of the ternary solution in the chamber above the membrane is greater than water density in the chamber under the membrane. For $\Delta C_2 > 0.35 \text{ mol}\cdot\text{l}^{-1}$ in curve 2B, J_{v2}^{B2} is linearly dependent on ΔC_2 with the same tangent of inclination angle as straight line 1B. In this case the density of ternary solutions in the chamber under the membrane is lower than water density above the membrane.

Graphs 1 and 2 presented in Figs. 5 and 6 were obtained when the solutions were mechanically stirred at 500 rpm. In this case flux J_{vs}^i is linearly dependent on ΔC_1 and/or ΔC_2 and it is not dependent on the gravitational configuration of the single-membrane system.

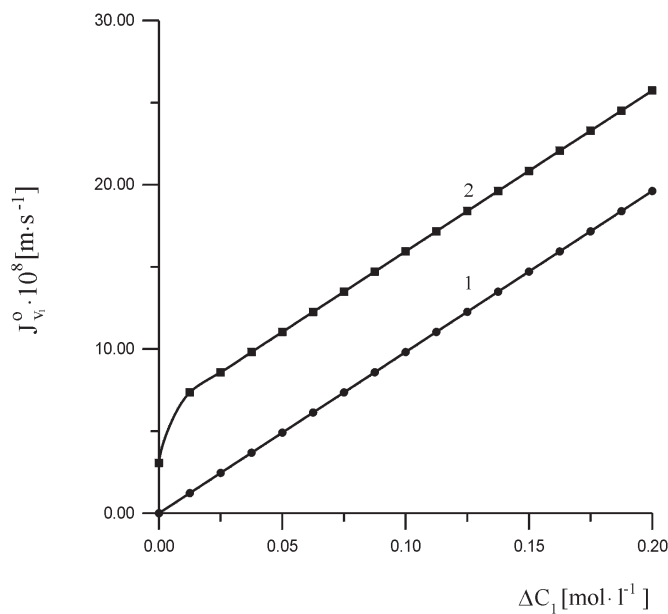


Figure 5. Experimental volume flux (J_{vs}^0) across a single-membrane osmotic-diffusive cell as a function of the potassium chloride concentration difference (ΔC_1) obtained under stirring conditions by mechanical means: graph 1, no ammonia; graph 2, $\Delta C_2 = 0.25 \text{ mol}\cdot\text{l}^{-1}$ ammonia.

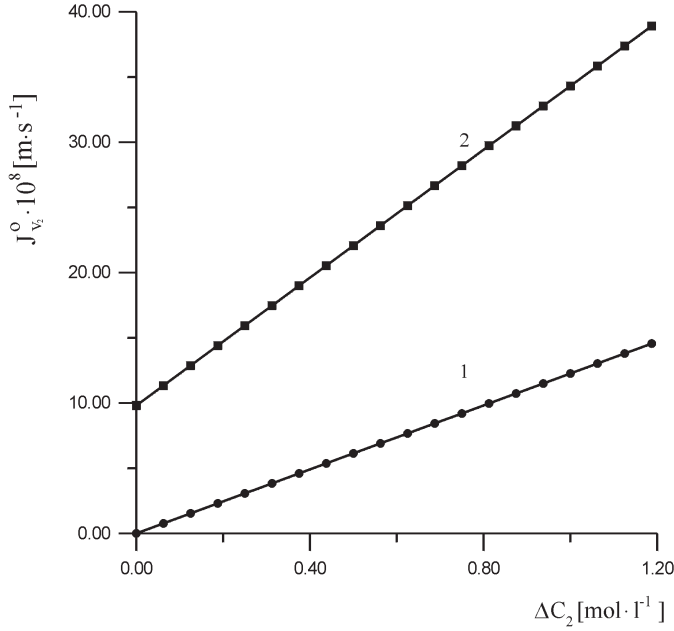


Figure 6. Experimental volume flux (J_{vs}^0) across a single-membrane osmotic-diffusive cell as a function of the ammonia concentration difference (ΔC_2) obtained under stirring conditions by mechanical means: line 1, no KCl; line 2, $\Delta C_2 = 0.1 \text{ mol}\cdot\text{l}^{-1}$ KCl.

c) Concentration dependencies of coefficients Ω_{11}^i and Ω_{22}^i for ternary solutions

In Fig. 7 the dependencies of coefficients Ω_{11}^i (upper graph) and Ω_{22}^i (lower graph) ($i = A_r, B_r$) on the concentration difference of potassium chloride (ΔC_1) were presented, with a constant concentration of ammonia ($\Delta C_2 = 0.25 \text{ mol}\cdot\text{l}^{-1}$) for configuration A_1 (lines 1A) and for configuration B_1 (lines 1B). From line 1A presented in the upper graph it implies that the value of coefficient $\Omega_{11}^{A_1}$ increases from value $\Omega_{11}^{A_1} = 0.78 \times 10^{-10} \text{ mol}\cdot\text{N}^{-1}\cdot\text{s}^{-1}$ to $\Omega_{11}^{A_1} = 0.9 \times 10^{-10} \text{ mol}\cdot\text{N}^{-1}\cdot\text{s}^{-1}$ and afterwards decreases nonmonotonically to $\Omega_{11}^{A_1} = 0.03 \times 10^{-10} \text{ mol}\cdot\text{N}^{-1}\cdot\text{s}^{-1}$, and for $\Delta C_1 \geq 0.1 \text{ mol}\cdot\text{l}^{-1}$, $\Omega_{11}^{A_1}$ is independent of ΔC_1 . From the curve 1B presented in the upper graph it implies that the value of coefficient $\Omega_{11}^{B_1}$ is initially constant and amounts to $\Omega_{11}^{B_1} = 0.03 \times 10^{-10} \text{ mol}\cdot\text{N}^{-1}\cdot\text{s}^{-1}$ and then from $\Delta C_1 = 0.0375 \text{ mol}\cdot\text{l}^{-1}$ it increases to value $\Omega_{11}^{B_1} = 0.56 \times 10^{-10} \text{ mol}\cdot\text{N}^{-1}\cdot\text{s}^{-1}$ and for $\Delta C_1 \geq 0.15 \text{ mol}\cdot\text{l}^{-1}$ it is independent of ΔC_1 . In the lower graph the dependencies of coefficients Ω_{22}^i on concentration differences of potassium chloride (ΔC_1) were presented, with a constant concentration of ammonia ($\Delta C_2 = 0.25 \text{ mol}\cdot\text{l}^{-1}$) for both configurations. From curve 1A we state that the value of coefficient $\Omega_{22}^{A_1}$ increases from value $\Omega_{22}^{A_1} = 0.78 \times 10^{-10} \text{ mol}\cdot\text{N}^{-1}\cdot\text{s}^{-1}$ to $\Omega_{22}^{A_1} = 0.9 \times 10^{-10} \text{ mol}\cdot\text{N}^{-1}\cdot\text{s}^{-1}$ and later decreases nonmonotonically to $\Omega_{22}^{A_1} = 0.01 \times 10^{-10} \text{ mol}\cdot\text{N}^{-1}\cdot\text{s}^{-1}$ and when $\Delta C_1 \geq$

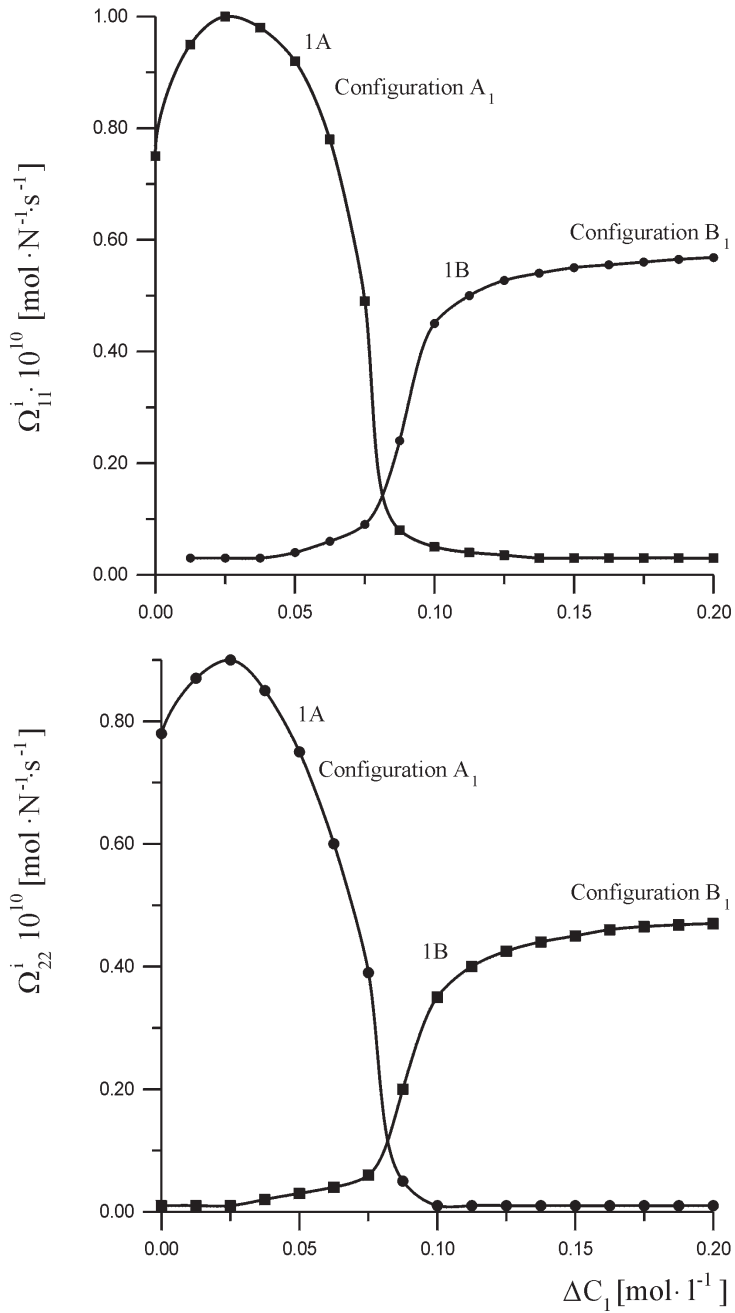


Figure 7. Potassium chloride concentration dependencies of Ω_{11}^i (upper graph) and Ω_{22}^i (lower graph) ($i = A_1, B_1$) in $0.25 \text{ mol} \cdot \text{l}^{-1}$ aqueous ammonia solution in configuration A₁ (curves 1A) and in configuration B₁ (curves 1B).

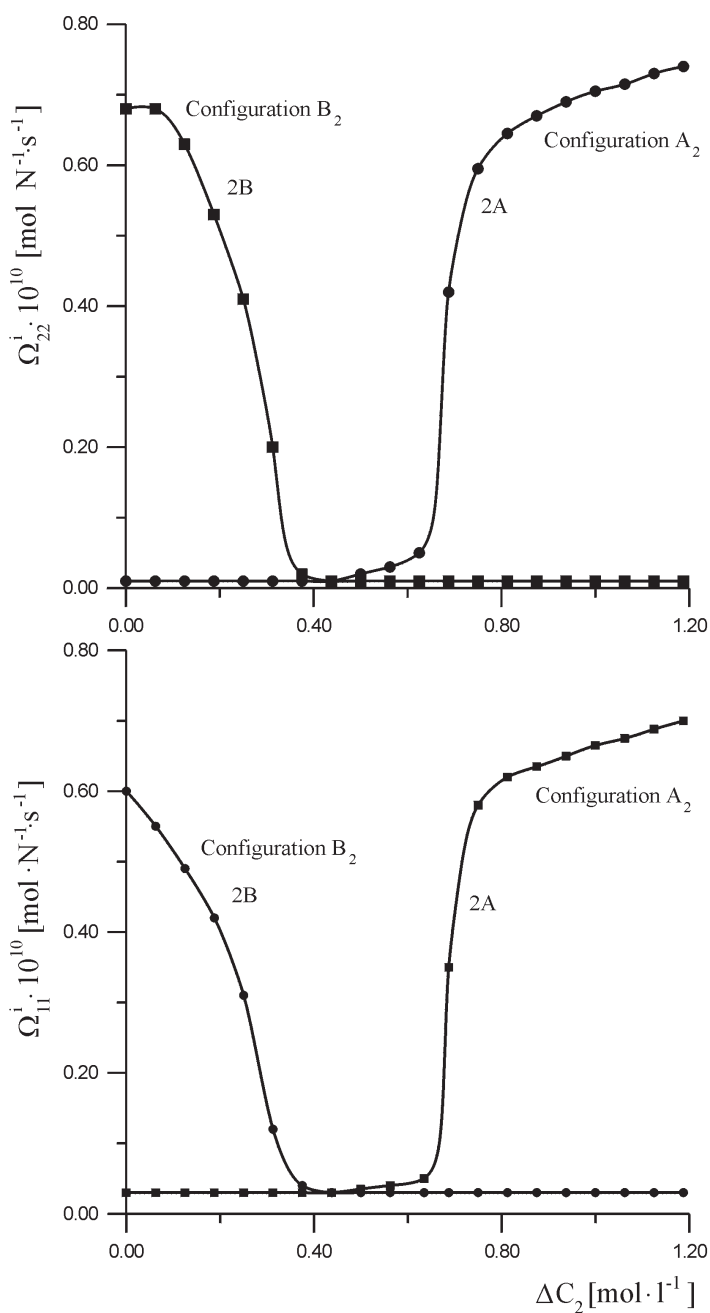


Figure 8. Ammonia concentration dependencies of Ω_{22}^i (upper graph) and Ω_{11}^i (lower graph) ($i = A_2, B_2$) in $0.1 \text{ mol} \cdot \text{l}^{-1}$ aqueous potassium chloride solutions in configuration A₂ (curves 2A) and in configuration B₂ (curves 2B).

0.1 mol·l⁻¹ it is independent on ΔC_1 . From curve 1B presented in this graph we find that the value of coefficient $\Omega_{22}^{B_1}$ is initially constant and amounts to $\Omega_{11}^{B_1} = 0.03 \times 10^{-10}$ mol·N⁻¹·s⁻¹ and then from $\Delta C_1 = 0.025$ mol·l⁻¹ it increases to value $\Omega_{11}^{B_1} = 0.48 \times 10^{-10}$ mol·N⁻¹·s⁻¹ and for $\Delta C_1 \geq 0.15$ mol·l⁻¹, value of $\Omega_{11}^{B_1}$ is not dependent on ΔC_1 .

In Fig. 8 the dependencies of coefficients Ω_{22}^i (upper graph) and Ω_{11}^i (lower graph) on concentration differences of ammonia (ΔC_2) were presented, with a constant concentration of potassium chloride ($\Delta C_1 = 0.1$ mol·l⁻¹) for configuration A₂ (curve 1A) and configuration B₂ (curve 1B). From curve 1A represented in the upper graph we see that the value of coefficient $\Omega_{22}^{A_2}$ is initially constant and amounts to $\Omega_{22}^{A_2} = 0.01 \times 10^{-10}$ mol·N⁻¹·s⁻¹ and then from $\Delta C_2 = 0.6$ mol·l⁻¹ it increases to a value of $\Omega_{22}^{A_2} = 0.65 \times 10^{-10}$ mol·N⁻¹·s⁻¹ (for $\Delta C_2 = 0.8$ mol·l⁻¹) and from there linearly, to value $\Omega_{22}^{A_2} = 0.8 \times 10^{-10}$ mol·N⁻¹·s⁻¹ (for $\Delta C_2 = 1.5$ mol·l⁻¹). When $\Delta C_2 > 1$ mol·l⁻¹, the value of $\Omega_{11}^{B_1}$ linearly increases with an increase in ΔC_2 . From curve 1B represented in this figure we know that the value of coefficient $\Omega_{22}^{B_2}$ decreases nonmonotonically from $\Omega_{22}^{B_2} = 0.68 \times 10^{-10}$ mol·N⁻¹·s⁻¹ to $\Omega_{11}^{B_2} = 0.01 \times 10^{-10}$ mol·N⁻¹·s⁻¹ and when $\Delta C_2 \geq 0.4$ mol·l⁻¹ it is independent of ΔC_2 . In the lower graph the dependencies of coefficients Ω_{11}^i on concentration differences of ammonia (ΔC_2) were presented with constant concentration differences of potassium chloride ($\Delta C_1 = 0.1$ mol·l⁻¹) for configuration A₂ (curve 2A) and configuration B₂ (curve 2B). From curve 2A it results that the value of coefficient $\Omega_{11}^{A_2}$ is initially constant and amounts to $\Omega_{11}^{A_2} = 0.03 \times 10^{-10}$ mol·N⁻¹·s⁻¹ and from $\Delta C_2 = 0.525$ mol·l⁻¹ it increases to $\Omega_{11}^{A_2} = 0.64 \times 10^{-10}$ mol·N⁻¹·s⁻¹ (for $\Delta C_2 = 0.8$ mol·l⁻¹) and then linearly, to value $\Omega_{11}^{A_2} = 0.75 \times 10^{-10}$ mol·N⁻¹·s⁻¹ (for $\Delta C_2 = 1.2$ mol·l⁻¹). From curve 2B presented in this graph we know that the value of coefficient $\Omega_{11}^{B_2}$ decreases nonmonotonically from value $\Omega_{11}^{B_2} = 0.6 \times 10^{-10}$ mol·N⁻¹·s⁻¹ to $\Omega_{11}^{B_2} = 0.04 \times 10^{-10}$ mol·N⁻¹·s⁻¹ and when $\Delta C_2 \geq 0.4$ mol·l⁻¹ is independent of ΔC_2 .

The dependencies of $\sigma_1^i(\Delta C_1, \Delta C_2)$ can be calculated from the formulae $\sigma_1^i = \sigma_1 \Omega_{11}^i (\omega_{11})^{-1}$, $\sigma_2^i = \sigma_2 \Omega_{22}^i (\omega_{22})^{-1}$ using data presented in Table 1 and Figs. 7 and 8.

d) The amplification of volume osmotic flux

In order to demonstrate the effect of the amplification of osmotic volume flux (J_{vs}^i), we take into consideration curves 1 (A,B) and 2 (A,B) shown in the Figs. 3 and 4. Lines 1A and 1B show that this same change in the value of concentration differences $\Delta(\Delta C_1)$ or $\Delta(\Delta C_2)$ in the case of binary solutions causes an identical change in the value of ΔJ_{vs}^i over the whole range of concentration differences ΔC_1 or ΔC_2 used. In the case of ternary solutions, illustrated by curves 2A and 2B, the same change in concentration differences causes different changes in ΔJ_{vs}^i with reference to its value and sign. The coefficient of the osmotic volume flux amplification (a_{vs}^i), specified by the equation given below is the quantitative measure of this effect

$$a_{vs}^i = \frac{(\Delta J_{vs}^i)_t}{(\Delta J_{vs}^i)_b} \quad (12)$$

where: $(\Delta J_{vs}^i)_t$ is the change in flux J_{vs}^i in ternary solutions, $(\Delta J_{vs}^i)_b$ is the change in flux J_{vs}^i in binary solutions, $s = 1, 2$.

In Figs. 9 and 10, the dependencies of coefficients a_{vs}^i ($i = A_r, B_r$ corresponding respectively to A_r and B_r configuration of single-membrane system, $r = 1, 2$) on the mean concentration \bar{C}_1 and a_{vs}^i on the mean concentration \bar{C}_2 are presented graphically. Curves 1A in these figures were obtained for configuration A_r , whereas curves 1B – for configuration B_r of single-membrane system. The calculation of concentrations \bar{C}_1 or \bar{C}_2 were carried out in the following way. If, for example, $\Delta C_k = C_k - C_o$ (where $k = 1, 2, 3, \dots, n$) then $\bar{C}_1 = (C_1 + C_o)/2$, $\bar{C}_2 = (C_2 + C_o)/2$, etc.

Curve 1A shown in Fig. 9 means that with an increase in \bar{C}_1 , coefficient $a_{v1}^{A_1}$ decreases non-monotonically from $a_{v1}^{A_1} = +120$ to minimal value of $a_{v1}^{A_1} = -130$, and then increases to a constant value of $a_{v1}^{A_1} = 1.5$, independent of \bar{C}_1 . A minimal value of $a_{v1}^{A_1} = -130$ was obtained for $\bar{C}_1 = 0.08 \text{ mol}\cdot\text{l}^{-1}$. From curve 1B in Fig. 9 we note that coefficient $a_{v1}^{B_1}$, for $\bar{C}_1 < 0.025 \text{ mol}\cdot\text{l}^{-1}$ is independent of \bar{C}_1 . For $\bar{C}_1 > 0.025 \text{ mol}\cdot\text{l}^{-1}$ coefficient $a_{v1}^{B_1}$ increases and for $\bar{C}_1 = 0.09 \text{ mol}\cdot\text{l}^{-1}$ it reaches a value of $a_{v1}^{B_1} = 4.5$. For $\bar{C}_1 > 0.15, \text{ mol}\cdot\text{l}^{-1}$ $a_{v1}^{B_1}$ does not depend on \bar{C}_1 and $a_{v1}^{B_1} = 1$.

From curve 2A shown in Fig. 10 it results that coefficient $a_{v2}^{A_2}$ for $\bar{C}_2 < 0.5 \text{ mol}\cdot\text{l}^{-1}$ is independent of \bar{C}_2 . For $\bar{C}_2 > 0.5 \text{ mol}\cdot\text{l}^{-1}$ coefficient $a_{v2}^{A_2}$ increases and for $\bar{C}_2 = 0.55 \text{ mol}\cdot\text{l}^{-1}$ it reaches value $a_{v2}^{A_2} = 16$. For $\bar{C}_2 > 0.8 \text{ mol}\cdot\text{l}^{-1}$, $a_{v2}^{A_2}$ does not depend on \bar{C}_2 and $a_{v2}^{A_2} = 3$. From curve 2B it results that with an increase in \bar{C}_2 , coefficient $a_{v2}^{B_2}$ decreases non-monotonically from $a_{v2}^{B_2} = +80$ to a minimal value of $a_{v2}^{B_2} = -370$, and then increases to a constant of $a_{v2}^{B_2} = 0.05$, independent of \bar{C}_2 . A minimal value of $a_{v2}^{B_2} = -370$ was obtained for $\bar{C}_2 = 0.25 \text{ mol}\cdot\text{l}^{-1}$.

Using equations (5) and (6), the equation (12) can be expressed in the following ways

$$a_{v1}^i = \frac{(\Delta J_{vs}^i)_{t1}}{(\Delta J_{vs}^i)_{b1}} = \frac{\xi_{vt}^i}{\xi_{vb}^i} \frac{1}{\Omega_{11}^i} \left\{ \Delta[\Omega_{11}^i(C_1)] + \Delta[\Omega_{22}^i(C_1)] \frac{\sigma_2}{\sigma_1} \frac{\zeta_t}{\zeta_b} \frac{\omega_{11}}{\omega_{22}} \frac{\Delta(\Delta C_2)}{\Delta(\Delta C_1)} \right\} \quad (13)$$

$$a_{v2}^i = \frac{(\Delta J_{vs}^i)_{t2}}{(\Delta J_{vs}^i)_{b2}} = \frac{\xi_{vt}^i}{\xi_{vb}^i} \frac{1}{\Omega_{22}^i} \left\{ \Delta[\Omega_{22}^i(C_2)] + \Delta[\Omega_{11}^i(C_2)] \frac{\sigma_1}{\sigma_2} \frac{\zeta_t}{\zeta_b} \frac{\omega_{22}}{\omega_{11}} \frac{\Delta(\Delta C_1)}{\Delta(\Delta C_2)} \right\} \quad (14)$$

where: $(\Delta J_{vs}^i)_{tk}$ is the change in flux J_{vs}^i in ternary solutions, and $(\Delta J_{vs}^i)_{bk}$ is the change in flux J_{vs}^i in binary solutions, $k = 1, 2$. In these equations $\Delta[\Omega_{11}^i(C_1)] = [\Omega_{11}^i(C_1)]_h - [\Omega_{11}^i(C_1)]_l$; $\Delta[\Omega_{22}^i(C_1)] = [\Omega_{22}^i(C_1)]_h - [\Omega_{22}^i(C_1)]_l$; $\Delta[\Omega_{22}^i(C_2)] = [\Omega_{22}^i(C_2)]_h - [\Omega_{22}^i(C_2)]_l$ and $\Delta[\Omega_{11}^i(C_2)] = [\Omega_{11}^i(C_2)]_h - [\Omega_{11}^i(C_2)]_l$. $\Delta[\Omega_{ss}^i(C_s)]$; $s = 1, 2$ are the changes in the values of the diffusion permeability coefficient in ternary solutions.

e) Volume flux graviosmotic effect

The flux graviosmotic effect $(jGOE)_s^i$ was determined on the basis of the measured values of J_{vs}^0 , $J_{vs}^{A_r}$ and $J_{vs}^{B_r}$ using equation (8). Concentration dependencies of $(jGOE)_1^i$ for binary (lines 1A and 1B) and ternary (lines 2A and 2B) solutions for

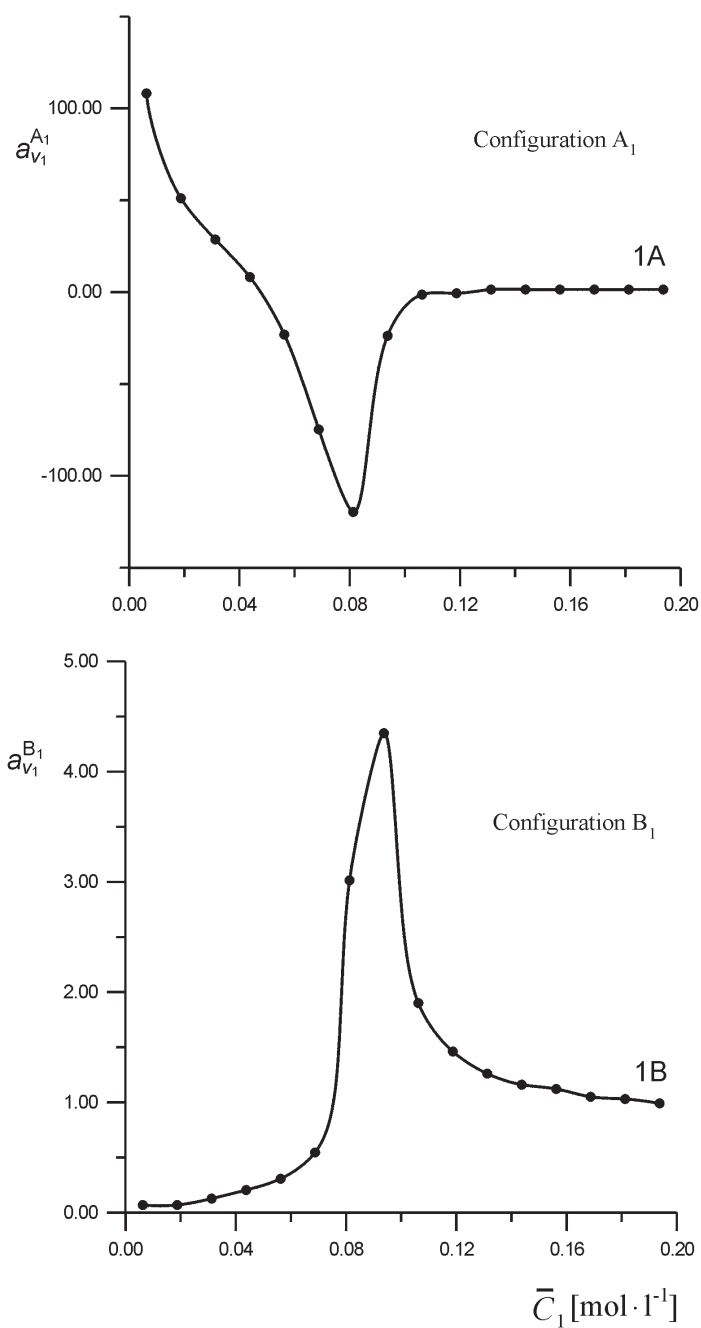


Figure 9. The amplification coefficient volume flux a_{v1}^i ($i = A_1, B_1$) as a function of the mean potassium chloride concentration (\bar{C}_1) in a $0.25 \text{ mol} \cdot \text{l}^{-1}$ aqueous ammonia solution for configuration A₁ (upper graph) and configuration B₁ (lower graph).

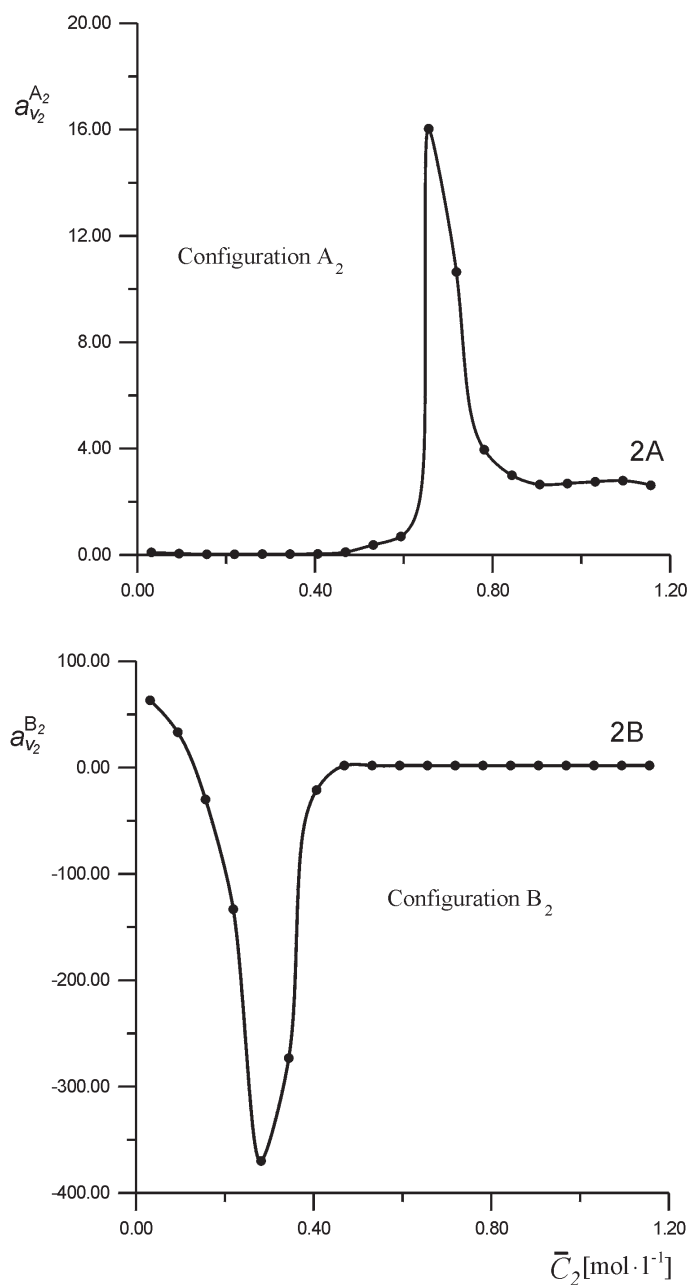


Figure 10. The amplification coefficient volume flux $a_{v_2}^i$ ($i = A_2, B_2$) as a function of the mean ammonia concentration (\bar{C}_2) in an ammonia in $0.1 \text{ mol}\cdot\text{l}^{-1}$ aqueous KCl solution for configuration A₂ (upper graph) and configuration B₂ (lower graph).

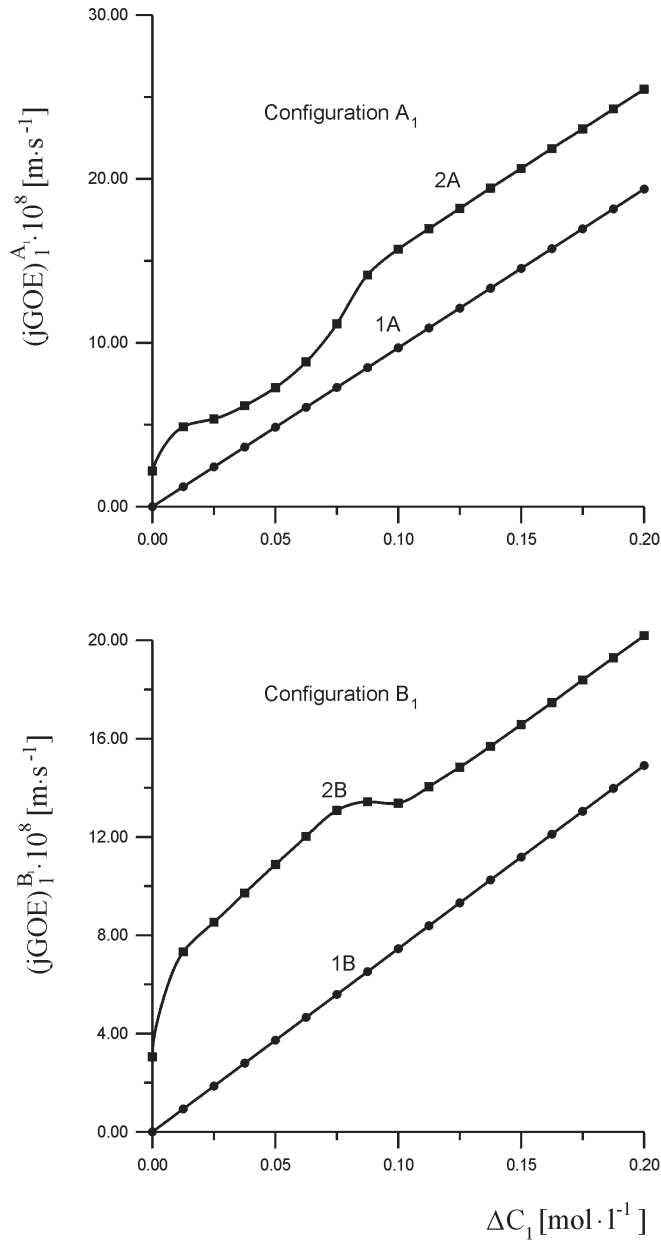


Figure 11. Experimental and calculated $(jGOE)_1^i$ as a function of the KCl concentration difference (ΔC_1) in binary (curves 1A and 1B) and in ternary solutions (curves 2A and 2B: curves 1A and 1B, no ammonia; curves 2A and 2B, $\Delta C_2 = 0.25 \text{ mol} \cdot \text{l}^{-1}$ ammonia solutions). Solid lines illustrate the $(jGOE)_1^i$ calculated on the basis of equation (23) after taking into consideration $\Omega_{11}^i(C_1)$ and $\Omega_{22}^i(C_1)$.

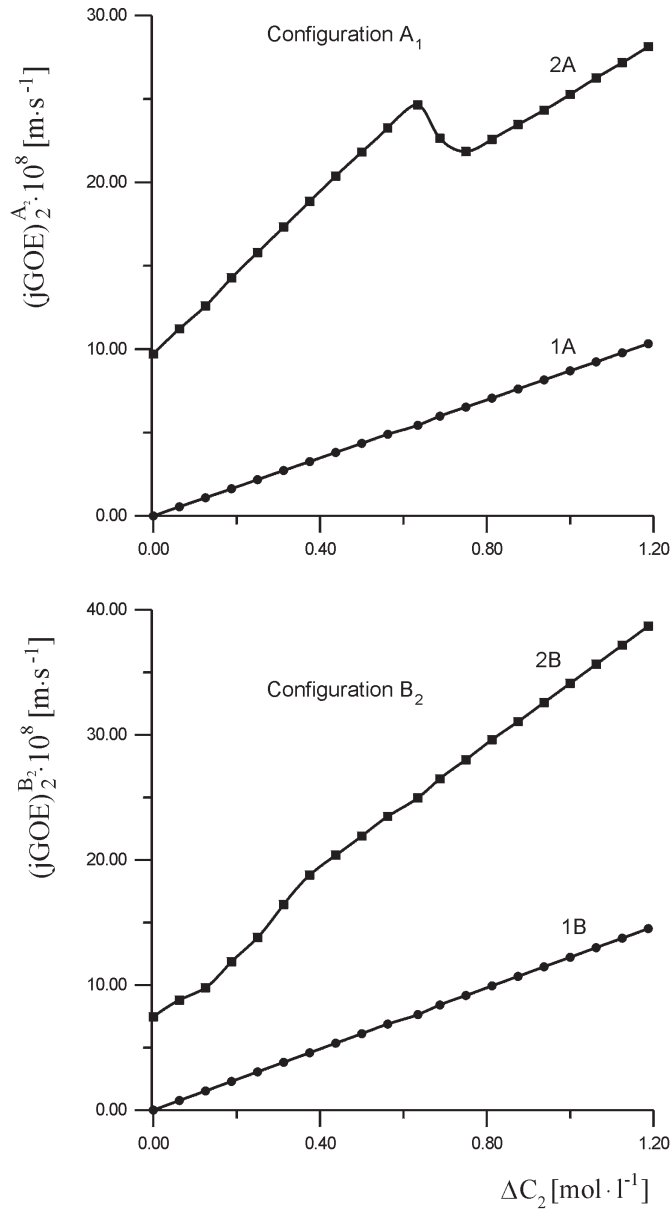


Figure 12. Experimental and calculated $(jGOE)_2^i$ as a function of the ammonia concentration difference (ΔC_2) in binary (curves 1A and 1B) and in ternary solutions (curves 2A and 2B): curves 1A and 1B, no KCl; curves 2A and 2B, $\Delta C_1 = 0.1 \text{ mol} \cdot \text{l}^{-1}$ KCl. Solid lines illustrate the $(jGOE)_2^i$ calculated using equation (24) after taking into consideration $\Omega_{22}^i(C_2)$ and $\Omega_{11}^i(C_2)$.

A_r and B_r configurations of single-membrane system are shown in Figs. 11 and 12. In Fig. 11, the dependencies of $(jGOE)_1^i$ ($i = A_1, B_1$) on concentration difference of potassium chloride (ΔC_1) with fixed concentration difference of ammonia (ΔC_2) are presented. Lines 1A and 1B were received for the $\Delta C_2 = 0 \text{ mol}\cdot\text{l}^{-1}$, the curves 2A and 2B for $\Delta C_2 = 0.25 \text{ mol}\cdot\text{l}^{-1}$. From this figure it clear that in the case of binary solutions $(jGOE)_1^i$ is linearly dependent on ΔC_1 and $(jGOE)_1^i$ in configuration A_1 is greater than in configuration B_1 . This also means that $(jGOE)_1^i$ is greater, when the solution with higher density is in the chamber above the membrane and water is below the membrane. Curve 2A shows that for $\Delta C_1 < 0.1 \text{ mol}\cdot\text{l}^{-1}$ the $(jGOE)_1^i$ increases nonlinearly, and for $\Delta C_1 > 0.1 \text{ mol}\cdot\text{l}^{-1}$ it increases linearly with increase in ΔC_1 . In this case, the density of ternary solution, in the chamber above the membrane, is higher than water density in the chamber below the membrane. Curve 2B shows that for both $0.0125 \text{ mol}\cdot\text{l}^{-1} < \Delta C_1 < 0.075 \text{ mol}\cdot\text{l}^{-1}$ and $\Delta C_1 > 0.1 \text{ mol}\cdot\text{l}^{-1}$ the $(jGOE)_1^i$ is linearly dependent on ΔC_1 . For $0.075 \text{ mol}\cdot\text{l}^{-1} < \Delta C_1 < 0.1 \text{ mol}\cdot\text{l}^{-1}$, $(jGOE)_1^i$ is nonlinearly dependent on ΔC_1 . In this case, the density of ternary solution in the chamber above the membrane is lower than water density in the chamber below the membrane.

In Fig. 12 the concentration dependencies of $(jGOE)_2^i$ for binary (lines 1A and 1B) and ternary (curves 2A and 2B) solutions for configurations A_2 and B_2 of single-membrane system are shown. In this figure, the dependencies of $(jGOE)_2^i$ on the concentration difference of ammonia (ΔC_2) with fixed concentration difference of potassium chloride (ΔC_1) are presented. Lines 1A and 1B were received for the $\Delta C_1 = 0 \text{ mol}\cdot\text{l}^{-1}$ and curves 2A and 2B for $\Delta C_1 = 0.1 \text{ mol}\cdot\text{l}^{-1}$. From this figure results that in the case of binary solutions $(jGOE)_2^i$ is linearly dependent on ΔC_2 and $(jGOE)_2^i$ in configuration A_2 is lower than in configuration B_2 . This also means that $(jGOE)_2^i$ is greater when the solution with higher density is in the chamber above the membrane, and water is below the membrane. Curve 2A shows that for $\Delta C_2 < 0.6 \text{ mol}\cdot\text{l}^{-1}$ the $(jGOE)_2^i$ is linearly dependent on ΔC_2 with the tangent of inclination angle 2.8-times greater than for line 1A. For $0.6 \text{ mol}\cdot\text{l}^{-1} < \Delta C_2 < 0.75 \text{ mol}\cdot\text{l}^{-1}$ $(jGOE)_2^i$ decreases nonlinearly with increase in ΔC_2 . For $\Delta C_2 > 0.75 \text{ mol}\cdot\text{l}^{-1}$, $(jGOE)_2^i$ is linearly dependent on ΔC_2 with the tangent of inclination angle 1.5-times greater than for line 1A. In this case, the density of ternary solutions in the chamber above the membrane is lower than water density in the chamber below the membrane. Curve 2B shows that for $\Delta C_2 < 0.4 \text{ mol}\cdot\text{l}^{-1}$ the $(jGOE)_2^i$ increases nonlinearly, and for $\Delta C_2 > 0.4 \text{ mol}\cdot\text{l}^{-1}$ it increases linearly with ΔC_2 . In this case, the density of ternary solutions in the chamber above the membrane is greater than water density in the chamber below the membrane.

Discussion

From the experimental data presented in this paper it results, that in the case of mechanically stirred binary and ternary electrolyte solutions osmotic volume flux is directly proportional to solution concentrations and does not depend on orientation

of membrane and measurement chamber with solution, relative to vector of gravitational force. Similar results for non-electrolyte solutions were obtained (Ślęzak and Dworecki 1984). In the case of mechanically unstirred binary electrolyte solutions osmotic volume flux is directly proportional to the solutions' concentration, and is strongly dependent on the sequence of solutions relative to the horizontal membrane orientation. The value of this flux is higher when the solution with a higher density is in the chamber above the membrane. In the case of ternary electrolyte solutions volume osmotic flux depends not only on the concentration and solution orientation relative to horizontally mounted membrane but also on solutions' composition. Therefore, this flux is a non-linear function of one solute concentration in solvent when the other solute concentration is constant.

These observations can be examined in terms of gravitational stability or instability of CBL. Through an extension of Rayleigh-Taylor stability analysis density gradients they were linked to a concentration gradient Rayleigh number R_C

$$R_C = \frac{g\alpha_C\beta_C d^4}{D_C\nu} \quad (15)$$

where: g is the gravitational acceleration, $\alpha_C = [(\partial\rho/\partial C)/\rho]$ the variation of density with concentration, $\beta_C = (\partial C/\partial z)$ the concentration gradient, d the solution depth along the gravitational (z) direction (the CBL thickness), D_C is a solute diffusion coefficient, ν is the kinematic viscosity. When $\alpha_C\beta_C$ is negative, i.e. the CBL is denser than the solution beneath it, convective instability occurs when R_C exceeds a critical value. This convection reduces CBL dimensions, thereby increasing transmembrane volume flux. A concentration-gradient Rayleigh number was used in a mathematical model for gravitationally sensitive volume flux (Ślęzak et al. 1985). Using the relation $\alpha_C\beta_C = (\rho - \rho_o)/(\rho_o d)$, R_C is given by

$$R_C = \frac{g(\rho - \rho_o)d^3}{D_C\nu\rho_o} \quad (16)$$

where ρ and ρ_o are the densities of solution and solvent, respectively.

Our investigations indicate that the values of the coefficients $\Omega_{k_s}^i$ for ternary solutions do depend on the solute concentrations and on the gravitational configuration of the single-membrane system. Regarding the expression (7) it is assumed that δ_1^i and δ_h^i varies with the gravitational stability, or instability of density gradient produced during volume flux. δ_1^i and δ_h^i are identified with d_1 and d_h , the characteristic length appearing in equations (15) and (16). Thus

$$\delta_1^i \approx d_1 = \left(\frac{R_C^i \nu_s^1 \rho_s^1 (D_s^1)^2}{gRT\Omega_s^i (\rho_s^h - \rho_s^1)} \right)^{\frac{1}{4}} \quad (17)$$

$$\delta_h^i \approx d_h = \left(\frac{R_C^i \nu_s^h \rho_s^h (D_s^h)^2}{gRT\Omega_s^i (\rho_s^h - \rho_s^1)} \right)^{\frac{1}{4}} \quad (18)$$

where: ν_s^l and ν_s^h are the kinematic viscosities of solutions in the compartments l and h respectively; ρ_s^l and ρ_s^h are the solution densities in compartments l and h respectively, R_C^i is the critical value of concentration Rayleigh number.

If we assume that CBL are symmetrical ($\delta_l^i = \delta_h^i = \delta_0^i$) and the coefficient D_s^i does not depend on the solution concentrations and on the gravitational direction, the ϑ_{ks}^i coefficient may be represented as

$$(\vartheta_{ks}^i)^4 - \left(4 + \chi \frac{(R_C)^i_k}{g(\rho_s^h - \rho_s^l)}\right) \vartheta_{ks}^i{}^3 + 6(\vartheta_{ks}^i)^2 - 4\vartheta_{ks}^i + 1 = 0 \quad (19)$$

where: $\vartheta_{ks}^i \equiv \frac{\Omega_{ks}^i}{\omega_{ks}}$, $\chi \equiv \frac{(RT)^3(\omega_s)^3}{(D_s)^2} \left[(\nu_s^l \rho_s^l)^{\frac{1}{4}} + (\nu_s^h \rho_s^h)^{\frac{1}{4}} \right]^4$.

The experimental values of ϑ_{ks}^i for ternary solutions, can be calculated from formula (11) using data presented in Table 1 and Figs. 7 and 8.

It appears from equation (6) that, in order to characterise the transport properties of a horizontally mounted membrane for ternary electrolyte solution, 19 coefficients are needed in practice. These parameters were defined in a previous paper (Ślęzak 1989). It appears from the results in Table 1 and from equation (6) that the values of the flux J_v^i are determined by the diagonal coefficients. The diagonal coefficients are greater than the non-diagonal coefficients by three orders of magnitude. Thus, this provides the basis for reduction of equation (6) accepting

$$\omega_{12} = \omega_{21} = \Omega_{12}^i = \Omega_{21}^i \approx 0 \quad (20)$$

Regarding the above condition, and the results presented in Figs. 3, 4, 5 and 6, equation (6) can be rewritten as

$$\begin{aligned} J_{v1}^i &= \xi_v^i [\vartheta_{11}^i(C_1)\sigma_1\zeta_1\Delta\Pi_1 + \vartheta_{22}^i(C_1)\sigma_2\zeta_2\Delta\Pi_2] \pm \Delta P \\ J_{v2}^i &= \xi_v^i [\vartheta_{22}^i(C_2)\sigma_2\zeta_2\Delta\Pi_2 + \vartheta_{11}^i(C_2)\sigma_1\zeta_1\Delta\Pi_1] \pm \Delta P \end{aligned} \quad (22)$$

where $\xi_v^i = L_p \{1 \mp (\omega_{11}\omega_{22})^{-1} L_p [\sigma_1\omega_{22}\bar{C}_1(\sigma_1 - \sigma_1^i) + \sigma_2\omega_{11}\bar{C}_2(\sigma_2 - \sigma_2^i)]\}^{-1}$.

In order to apply this equation to a description of transmembrane transport in ternary solutions, the assumption of the Ω_{11}^i and Ω_{22}^i coefficients being dependent on the concentration and configuration is required. The pertinence of the above assumption is confirmed by the data on Ω_{11}^i and Ω_{22}^i in ternary solutions, shown in Figs. 7 and 8. Taking into consideration dependence of the coefficients Ω_{11}^i and Ω_{22}^i , demonstrated in these figures and the values for the membrane parameters listed in Table 1, the values of J_{v1}^i and J_{v2}^i as functions of the concentration differences ΔC_1 and ΔC_2 were calculated on the basis of equations (21) and (22). The solid lines in Figs. 3 and 4 present the results calculated for J_{v1}^i and J_{v2}^i . One observes good agreement between the experimental data and the results of calculation. Therefore, equations (21) and (22), after taking into consideration the concentration depen-

dence of $\Omega_{11}^i(C_1)$, $\Omega_{11}^i(C_2)$, $\Omega_{22}^i(C_2)$, and $\Omega_{22}^i(C_1)$, yield satisfactory curve fitting to the experimental results.

If we assume that J_{vs}^i is the generalized flux and ΔC_s is a generalized thermodynamic force, the regions where $[dJ_{vs}^i/d(\Delta C_s)] < 0$ can be classified as the negative differential resistance regions. This phenomenon appears in nature and constitutes a very important factor in the physics of semiconductors (Weber and Ford 1970), membranology (Anderson 1978) and biophysics (Cole 1968). If in the non-linear element there is a negative resistance region, then in this element the generation of electrical and/or mechanical oscillation may appear. Examples of this behaviour are Teorell's membranous oscillator (Teorell 1959), semiconductor generator (Krause 1976) and electrical oscillations in excitable tissues (Cole 1968).

The non-linear characteristics $J_{vs}^i = f(\Delta C_s)$ presented in Figs. 3 and 4 (curves 2A and 2B) show that the single-membrane system, which contains the ternary ionic solutions under investigation is determined by a non-linear element. In the case of the characteristic $J_{v1}^{A1} = f(\Delta C_1)$, for $0.05 \text{ mol}\cdot\text{l}^{-1} < \Delta C_1 < 0.1 \text{ mol}\cdot\text{l}^{-1}$, the condition $[\Delta J_{v1}^{A1}/\Delta(\Delta C_1)] < 0$ is fulfilled. If ΔC_1 accomplishes the relation $0 \text{ mol}\cdot\text{l}^{-1} < \Delta C_1 < 0.05 \text{ mol}\cdot\text{l}^{-1}$ or $\Delta C_1 > 0.1 \text{ mol}\cdot\text{l}^{-1}$, the condition $[\Delta J_{v1}^{A1}/\Delta(\Delta C_1)] \geq 0$ is satisfied. In case of characteristic $J_{v1}^{B1} = f(\Delta C_1)$, for all values of ΔC_1 , we can write a condition where $[\Delta J_{v1}^{B1}/\Delta(\Delta C_1)] \geq 0$. Similarly, in a case where characteristic $J_{v2}^{A2} = f(\Delta C_2)$, for all values of ΔC_2 , the condition $[\Delta J_{v2}^{A2}/\Delta(\Delta C_2)] \geq 0$, is fulfilled. Then, if characteristic $J_{v2}^{B2} = f(\Delta C_2)$, for $0.1 \text{ mol}\cdot\text{l}^{-1} < \Delta C_2 < 0.3 \text{ mol}\cdot\text{l}^{-1}$, the condition $[\Delta J_{v2}^{B2}/\Delta(\Delta C_2)] < 0$ is satisfied. If ΔC_2 accomplishes the relation $0 \text{ mol}\cdot\text{l}^{-1} < \Delta C_2 < 0.1 \text{ mol}\cdot\text{l}^{-1}$ or $\Delta C_2 > 0.3 \text{ mol}\cdot\text{l}^{-1}$, the relation $[\Delta J_{v2}^{B2}/\Delta(\Delta C_2)] \geq 0$ is fulfilled.

Using the equations, equation (9) is regarded as the model equation for the volume flux graviosmotic effect. Accepting the condition (20) and that the coefficients Ω_{11}^i and Ω_{22}^i are dependent on concentrations C_1 and C_2 , we obtain

$$(jGOE)_1^i = [L_p\sigma_1 - \xi_v^i\vartheta_{11}^i(C_1)]\zeta_1\Delta\Pi_1 + [L_p\sigma_2 - \xi_v^i\vartheta_{22}^i(C_1)]\zeta_2\Delta\Pi_2 + (\xi_v^i - L_p)\Delta P \quad (23)$$

$$(jGOE)_2^i = [L_p\sigma_2 - \xi_v^i\vartheta_{22}^i(C_2)]\zeta_2\Delta\Pi_2 + [L_p\sigma_1 - \xi_v^i\vartheta_{11}^i(C_2)]\zeta_1\Delta\Pi_1 + (\xi_v^i - L_p)\Delta P \quad (24)$$

where $\xi_v^i = L_p\{1 - (\omega_{11}\omega_{22})^{-1}L_p[\sigma_1\omega_{22}(\tilde{C}_1^i(1 - \sigma_1^i) - (1 - \sigma_1)\tilde{C}_1) + \sigma_2\omega_{11} \cdot (\tilde{C}_2^i(1 - \sigma_2^i) - (1 - \sigma_2)\tilde{C}_2^i)]\}^{-1}$.

We have obtained equations, including parameters Ω_{ks}^i , which refer to concentration boundary layers. These equations can be used to analyse the volume flux graviosmotic effect. Taking into consideration the above equations the values of coefficients listed in Table 1 and in Figs. 7 and 8 the $(jGOE)_1^i$ and $(jGOE)_2^i$ were calculated for configurations A_r and B_r and binary and ternary solutions. The calculated results are illustrated by full lines in Figs. 11 and 12.

Conclusion

Inferences in the conducted investigations show that:

1. The experimental data presented in this paper indicate that gravitational force has essential influence on volume osmotic flow electrolyte solutions. As was pointed out, the measure of this influence is volume flux graviosmotic effect $(jGOE)_s^i$. The values of $(jGOE)_s^i$ depend on the sequence of solution position relatively to a given membrane, located perpendicularly to the direction of gravitational force and on a composition and concentration of solutions separated by the membrane. The situation in which the solutions are mechanically stirred, that is homogeneous with respect to the concentration, illustrates a situation in which gravitational force has an influence on passive membrane transport, because it does not create or eliminate local concentration gradients. The situation is possible in a biological system under hypergravity conditions.

2. In case of the lack of mechanical stirring of solutions, on both sides of the membrane, concentration boundary layers are created. Only in a situation where the density gradient vector is opposite to gravitational force in the area near the membrane does the natural convection appear and causes weak solution stirring. Such a situation could occur in biological systems, present in the Earth's gravitational field (Müller et al. 1984). A state devoid of natural convection responds to microgravity (hypogravity) conditions. This is the situation when the cell membrane is not proven with nutrients. This means, that in the close vicinity of the cell membrane the concentration of nutrients is minimal. In a state of zero convection $(jGOE)_s^i$ obtains maximal values, increasing with an increase in solution concentration. Moreover in a state without convection $(jGOE)_s^i \approx J_{vs}^0$, this means that the absence of gravitational force hampers passive membrane transport in a state of zero convection almost totally, followed by the convective state $jGOE < J_{vs}^0$.

3. The experimental results presented in this paper can be important for the recognition of the influence of the mechanism of hypo- and hypergravity on passive transmembrane transport in biological systems.

4. Single-membrane systems are characterised by amplification of volume flux. This effect is the result of the presence of gravitation and/or destruction of concentration boundary layers. The effect of amplification of the volume flux is an indication of a new osmotic property in a single-membrane system. It may be added to a group of regulatory effects, including phenomena such as rectification, amplification and oscillation of transmembrane flows.

5. It has been demonstrated herein that the model equations for the $(jGOE)_s^i$ may be used in interpreting data related to the volume flux graviosmotic effect in a single-membrane osmotic-diffusive cell. However, this is possible only when the dependence of Ω_{ks}^i on concentration is known. Values of these parameters are governed by the hydrodynamic state of the concentration boundary layers complex.

Acknowledgements. Part of the support for A. Ślęzak and J. Wąsik was provided by the KBN grant No. 2PO 3B 13919.

References

- Anderson J. E. (1978): Model for Current-Controlled Negative Resistance in Ion/Membrane System. *J. Membr. Sci.* **4**, 35—40
- Barry P. H., Diamond J. M. (1984): Effects of Unstirred Layers on Membrane Phenomena, *Physiol. Rev.* **64**, 763—872
- Bhattacharya S., Hwang S. T. (1997): Concentration polarization, separation factor, and Pecelt number in membrane processes. *J. Membr. Sci.* **132**, 73—90
- Cogoli A., Gmünder F. K. (1991): Gravity effects on single cells: techniques, findings and theory. *Adv. Space Biol. Med.* **1**, 183—248
- Cole K. S. (1968): Membranes, ions and impulses, University of California Press, Berkeley
- Cotton U. C., Reuss L. (1989): Measurement of the effective thickness of mucosal unstirred layer in *Necturus* gallbladder epithelium. *J. Gen. Physiol.* **93**, 631—647
- Dainty J. (1963): Water relations in plants cells. *Adv. Bot. Res.* **1**, 279—326
- Dainty J., House C. R. (1966): Unstirred layer in frog skin. *J. Physiol. (London)* **182**, 66—78
- Dworecki K. (1995): Interferometric Investigations of Near-Membrane Diffusion Layers. *J. Biol. Phys.* **21**, 37—49
- Dworecki K., Waśik S. (1997): The investigation of time-dependent solute transport through horizontally situated membrane: the effect of configuration membrane system. *J. Biol. Phys.* **23**, 181—195
- Ginzburg B. Z., Katchalsky A. (1963): The Frictional Coefficients of the Flows of Non-Electrolytes Through Artificial Membranes. *J. Gen. Physiol.* **47**, 403—418
- Havstein B. (1987): Kinetics of formation of a flow-inhibiting boundary layer in liquid-solid filtration. *Chem. Eng. J.* **35**, 123—136
- Hughes-Fulford M. (1993): Review of the biological effects of weightlessness on the human endocrine system. *Receptor* **3**, 145—154
- Hwang S. T., Kammermeyer K. (1981): Membranes in Separations. John Wiley & Sons/Interscience, New York
- Inenaga K., Yoshida N. (1980): Effect of an unstirred layer on ion transport through a membrane. *J. Membr. Sci.* **6**, 271—282
- Kargol M. (1992): The graviosmotic hypothesis of xylem transport of water in plants. *Gen. Physiol. Biophys.* **11**, 469—487
- Kargol M. (1994): Full analytical description of graviosmotic volume flows. *Gen. Physiol. Biophys.* **13**, 109—126
- Katchalsky A., Curran P. F. (1965): Nonequilibrium Thermodynamics in Biophysics. Harvard University Press, Cambridge
- Krause P. C. (1976): Analysis of Electric Machinery. McGraw-Hill, Inc., New York
- Lerche D., Wolf H. (1971): Laserinterferometrische Bestimmung der Diffusionsschicht an Ionensustauuchmembranen. *Studia Biophys.* **27**, 189—197
- Lerche D. (1976): Temporal and local concentrations changes in diffusion layers at cellulose membranes due to concentrations differences between the solutions on both sides of the membranes. *J. Membr. Biol.* **27**, 193—205
- Müller S. C., Plessner Th., Hess B. (1984): Hydrodynamic Instabilities and Pattern Formation in a Cytoplasmic Medium from Yeast. *Naturwissenschaften* **71**, 637—638
- Nernst W. (1904): Theorie der Reaktionsgeschwindigkeit in heterogenen Systemen. *Z. Phys. Chem.* **47**, 52—63
- Pedley T. J., Fischbarg J. (1978): The development of osmotic flow through an unstirred layer. *J. Theor. Biol.* **70**, 426—446
- Pedley T. J., Fischbarg J. (1980): Unstirred layer effects in osmotic water flow across gall-bladder. *J. Theor. Biol.* **54**, 89—102

- Pedley T. J., (1983): Calculation of unstirred layer thickness in membrane transport experiments: a survey. *Q. Rev. Biophys.* **16**, 115—150
- Pohl P., Saparov S. M., Antonenko Y. N. (1997): The effect of a transmembrane osmotic flux on the ion concentration distribution in the immediate membrane vicinity measured by microelectrodes. *Biophys. J.* **72**, 1711—1718
- Przestalski S., Kargol M. (1987): Gravidiosis. *Com. Molec. Cell Biophys.* **4**, 249—264
- Rautenbach R., Albert R. (1989): *Membrane Processes*. Wiley, Chichester
- Schatz A., Linke-Hommes A. (1989): Gravity and the Membrane-Solution Interface: Theoretical Investigations. *Adv. Space Res.* **11**, 61—64
- Schatz A., Reitstetter R., Briegleb W., Linke-Hommes A. (1992): Gravity effects on membrane processes. *Adv. Space Res.* **12**, 51—53
- Ślęzak A. (1989): Irreversible thermodynamic model equations of the transport across a horizontally mounted membrane. *Biophys. Chem.* **34**, 91—102
- Ślęzak A. (1990): A model equations for the gravielectric effect in electrochemical cells. *Biophys. Chem.* **38**, 189—199
- Ślęzak A. (1997): A Model Equation for the Electric Current in a Single-Membrane Electrochemical Cell and Heterogeneous Ionic Solutions. *Ann. Acad. Med. Siles.* **33**, 267—273
- Ślęzak A., Dworecki K. (1984): Asymmetry and Amplification of Osmotic Flows of Non-Electrolytes in One-Membrane System. *Studia Biophys.* **100**, 21—48
- Ślęzak A., Dworecki K., Anderson J. E. (1985): Gravitational effects on transmembrane flux: the Rayleigh-Taylor convective instability. *J. Membr. Sci.* **23**, 71—81
- Ślęzak A., Turczyński B., Nawrat Z. (1989): Modification of the Kedem-Katchalsky-Zelman model-equations of the transmembrane transport. *J. Non-Equilib. Thermodyn.* **14**, 205—218
- Ślęzak A., Wąsik J., Dworecki K. (2000a): Gravitational effects in a passive transmembrane transport: the flux graviosmotic and gravidiffusive effects in non-electrolytes. *J. Biol. Phys.*, **26**, 149—170
- Ślęzak A., Jasik-Ślęzak J., Sieroń A. (2000b): Gravitational effects in passive osmotic flows across polymeric membrane of electrolytic solutions. *Polim. Med.* **30**, 21—44
- Teorell T. (1959): Electrokinetic Membrane Process in Relation Properties of Excitable Tissues. *J. Gen. Physiol.* **42**, 831—863.
- Thomson A. B., Dietchy J. M. (1977): Derivation of the equations that describe the effects of unstirred water layer on the kinetic parameters of active process in the intestine. *J. Theor. Biol.* **64**, 277—294
- Thorney J. H. (1976): *Mathematical Models in Plant Physiology*. Academic Press, London
- Weber W. H., Ford G. W. (1970): Double injection in semiconductors heavily doped with deep two-level traps. *Solid-State Electro.* **13**, 1333—1356

Final version accepted: November 28, 2001